

Reconfigurable Intelligent Surface Aided Communications: Asymptotic Analysis under Imperfect CSI

Bayan Al-Nahhas, *Student Member, IEEE*,

Qurrat-Ul-Ain Nadeem, *Member, IEEE*, and Anas Chaaban, *Senior Member, IEEE*

Abstract

This work studies the asymptotic sum-rate performance of a multi-user reconfigurable intelligent surface (RIS) assisted-multiple-input single-output (MISO) downlink system under imperfect CSI and Rayleigh and Rician fading. We first extend the existing least squares (LS) ON/OFF channel estimation protocol to a multi-user system, where we derive minimum mean squared error (MMSE) estimates of all RIS-assisted channels over multiple sub-phases. We also consider a low-complexity direct estimation (DE) scheme, where the BS obtains the MMSE estimate of the overall channel in a single sub-phase. Under both protocols, the BS implements maximum ratio transmission (MRT) precoding while the RIS phases are studied in the large system limit, where we derive deterministic equivalents of the signal-to-interference-plus-noise ratio (SINR) and the sum-rate. The derived asymptotic expressions reveal that under Rayleigh fading, the RIS phase-shift values do not play a significant role in improving the sum-rate but the RIS still provides an array gain. However, under Rician fading, we show that RIS provides both array and reflect beamforming gains. A projected gradient ascent-based algorithm is used to optimize the phase-shifts under both ON/OFF and DE protocol. Simulation results show that the DE of the overall channel yields better downlink performance when considering large systems.

I. INTRODUCTION

The massive connectivity, high speed and low latency promised by the Fifth Generation (5G) and beyond communication networks will enable instantaneous connectivity to billions of devices, resulting in a truly connected world. Various technological advances, including

The authors are with School of Engineering, The University of British Columbia, Kelowna, Canada. (e-mail: bayanalnahhas@gmail.com, {qurrat.nadeem, anas.chaaban}@ubc.ca). Parts of this paper has been presented in [1].

massive multiple-input multiple-output (MIMO), millimeter wave (mmWave) communication, and network densification, are leading the emergence of 5G networks. Their advantages are indisputable, but they face two main practical limitations. First, they consume a lot of power and incur high hardware deployment costs which are critical issues for practical implementation [2], [3], and second, they struggle to provide quality of service guarantee in harsh propagation environments. For example, the high path loss especially at mmWave frequencies limits the network coverage, poor scattering results in rank-deficient MIMO channels, while anomalous reflections and refractions from environmental objects result in uncontrollable interference.

In light of these limitations, an important challenge has been to find a way to control the propagation of radio waves in the environment in an energy-efficient way to improve the system performance without increasing the power consumption, resulting in green and sustainable future wireless networks. A transformative solution that addresses this need is deploying reconfigurable intelligent surfaces (RISs), also known as intelligent reflecting surfaces (IRSs) [4]–[7], on objects in the environment to customize the propagation of radio waves through controlled reflections. In the recent literature on this concept, RIS is abstracted as a planar array of a large number of passive reflecting elements, where each element can be independently reconfigured to induce a desired phase-shift onto the incident electromagnetic waves. By properly adjusting the phase-shifts induced by all passive elements of the RIS, desired communication objectives can be realized [7], [8]. Current implementations of RISs include reflect-arrays and reconfigurable meta-surfaces, which can manipulate the incident waves in a passive manner without generating new radio signals and therefore without incurring any notable power consumption.

Motivated by these remarkable advantages, various works on RIS-assisted systems have appeared that focus on the design of the reflect beamforming at the RIS to meet different objectives. In [9], the authors formulate and solve the sum-rate maximization problem for the RIS-assisted multiple-input single-output (MISO) system by jointly optimizing the active beamforming (precoding) at the BS and passive reflect beamforming at the RIS. In [10], [11], Wu *et al.* optimize the precoding at the BS and reflect beamforming at the RIS under the criteria of minimizing the total transmit power at the BS, subject to users' individual SINR constraints. They further extend their work in [12] to solve a similar optimization problem under discrete RIS phase-shifts. The work in [13] aims at maximizing the minimum SINR of an RIS-assisted MISO system in the asymptotic regime. RISs have also found applications in UAV communication [14] and NOMA systems [15], respectively. Moreover, the use of RISs to enable indoor communication in the

presence of blockages has been the subject of [16], [17].

Most of the current literature on RIS-assisted systems focuses on solving optimization problems while assuming perfect channel state information (CSI) to be available at the BS and the RIS. Channel estimation is a practical challenge in RIS-assisted communication systems since the RIS elements have no radio hardware or software that enable them to send or receive pilot symbols and to estimate the RIS-assisted links. Recently some works have proposed channel estimation protocols to estimate the RIS-assisted channels taking into account the radio limitations of the RIS [18]–[23]. Least-square channel estimates based on pilot training have been proposed in [18]–[20] for a single-user system while channel estimation algorithms that exploit the sparsity of the cascaded channel matrix comprising of the BS-to-RIS link and the RIS-to-user link have been proposed for a multi-user system in [21], [22]. However, most of these works only focus on developing the channel estimation protocols and do not utilize the derived estimates or algorithms in the design and analysis of the RIS-assisted system. Moreover, the protocols that yield closed-form expressions for the estimates [18]–[20], [23] require the channel training time to grow prohibitively large with number of RIS elements.

In light of these limitations, our goal in this work is to study the sum-rate performance of an RIS-assisted MISO system under imperfect CSI by developing channel estimation protocols and using the estimates to evaluate the end-to-end performance. Channel estimation is performed by either estimating all individual RIS-assisted links (BS-user and the cascaded BS-RIS-user links) requiring long training times, or directly estimate the overall BS-user channel as done in a conventional MISO system. Specifically, we consider a multi-user RIS-assisted downlink MISO system where the BS-RIS channel is LoS, since the RIS is assumed to be deployed at a high altitude and thus the path between the BS and the RIS is fading-free due to lack of obstructions and scatterings [11], [13], [23], while RIS-users channels and BS-users direct channels undergo Rayleigh or Rician fading. We then extend the ON/OFF estimation scheme from [18] to a multi-user system and derive the minimum mean square error (MMSE) estimates of all the direct and RIS-assisted channels over multiple sub-phases. Recognizing the large overhead imposed by this protocol, we also propose a direct estimation (DE) scheme in which the BS estimates the overall BS-user channel in one sub-phase, instead of estimating the individual links over multiple sub-phases. The derived estimates are used to implement maximum ratio transmission (MRT) precoding at the BS. While the DE protocol is not very practical in the non-asymptotic regime where we need estimates of all individual RIS-assisted channels to design the RIS [18], it

can be a viable scheme for large systems, where the SINR and sum-rate approach deterministic quantities that do not depend on instantaneous channels.

To design the RIS parameters, we resort to the asymptotic analysis of the sum-rate motivated by the large system sizes envisioned for future networks. Specifically, we develop deterministic equivalents of the SINR and sum-rate under both estimation protocols, which become tight in the large system limit [24]. Under Rayleigh fading RIS-to-users channels, the derived deterministic equivalents reveal that RIS phase-shifts do not matter asymptotically and optimizing them yields no noticeable performance gain. Applying the results to a special case from [25], we find that while RIS yields no significant reflect beamforming gain under Rayleigh fading, it does yield an array gain which becomes significant in noise-limited systems. Under Rician fading, however, the RIS phase-shifts appear explicitly in the deterministic equivalents and therefore RIS yields both an array gain and reflect beamforming gain asymptotically. The RIS phase-shifts are optimized utilizing the developed deterministic equivalents under both ON/OFF and DE protocols using projected gradient ascent. Simulation results verify the derived insights and illustrate the excellent match yielded by deterministic equivalents. Moreover, we observe that if the RIS is designed using only statistical CSI by relying on the derived deterministic equivalents, we do not need estimates of all individual RIS-assisted links, and the DE scheme becomes desirable due to the reduction in channel training time.

The rest of the paper is organized as follows. In Section II, we present the system and channel models. In Section III, we develop the MMSE ON/OFF and MMSE DE protocols under both Rayleigh and Rician fading. Section IV presents the asymptotic analysis of the SINR and sum-rate and develops optimization algorithms to design the RIS phase-shifts. Simulation results are provided in Section V, and Section VI concludes the paper.

Notation: Scalars are denoted by italic letters, while vectors are denoted by bold letters. The identity matrix of size $N \times N$ is denoted by \mathbf{I}_N , and $\mathbf{1}_N$ denote to an $N \times 1$ ones vector. The imaginary unit of a complex number is denoted by j with $j = \sqrt{-1}$. The superscripts $(\cdot)^*$, $(\cdot)^T$, and $(\cdot)^H$ denote the complex conjugate, transpose, and Hermitian transpose, respectively. $\mathbb{E}\{\cdot\}$ and $\text{Var}\{\cdot\}$ denote the expectation and variance of a random variable. The circularly symmetric Gaussian distribution with mean μ and variance σ^2 is denoted by $\mathcal{CN}(\mu, \sigma^2)$ and $\text{diag}(\mathbf{q})$ is the diagonal matrix whose main diagonal is given by \mathbf{q} . The Euclidean norm of vector \mathbf{q} is $\|\mathbf{q}\|$.

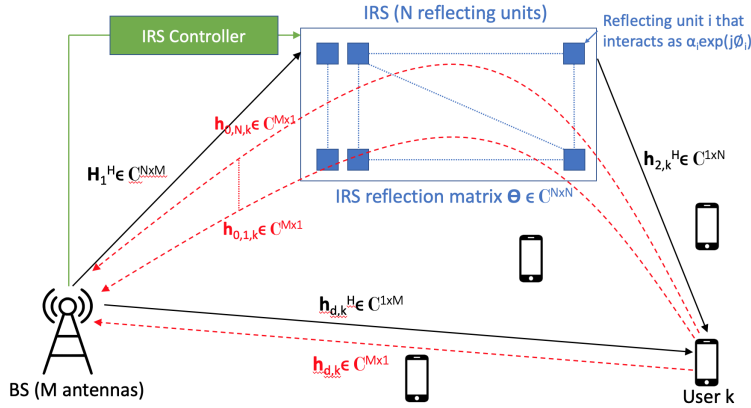


Fig. 1: Sketch of RIS-assisted MISO system. The black arrows denote the downlink channels between BS-RIS, RIS-User and BS-User, while the red dotted lines denote the corresponding uplink channels.

II. SYSTEM MODEL

In this section, we present the transmission model for the considered RIS-assisted downlink multi-user MISO system.

A. Signal Model

As shown in Fig. 1, we consider an RIS-assisted MISO communication model where a BS equipped with M antennas, communicates with K single antenna users. An RIS composed of N passive reflecting elements is installed in the LoS of the BS and assists it in communicating with the users. Equipped with a smart controller, the RIS can dynamically adjust the phase-shift induced by each reflecting element on the impinging electromagnetic waves. We consider a time-division duplex protocol and assume transmission over flat-fading channels. The received baseband signal y_k at user k is given as,

$$y_k = \mathbf{h}_k^H \mathbf{x} + n_k, \quad (1)$$

where the channel \mathbf{h}_k is the end-to-end channel between the BS and user k , n_k is the noise received at the user's end, and $\mathbf{x} = \sum_{k=1}^K \sqrt{p_k} \mathbf{g}_k s_k$ is the transmit (Tx) signal vector, where $\mathbf{g}_k \in \mathbb{C}^{M \times 1}$, $p_k > 0$, and $s_k \sim \mathcal{CN}(0, 1)$ are the precoding vector, signal power, and data symbol for user k , respectively. The Tx vector satisfies the average constraint

$$\mathbb{E}[||\mathbf{x}||^2] = \text{tr}(\mathbf{P}\mathbf{G}^H\mathbf{G}) \leq P_{max}, \quad (2)$$

where P_{max} is the Tx power budget, $\mathbf{P} = \text{diag}(p_1, \dots, p_K)$, and $\mathbf{G} = [\mathbf{g}_1, \mathbf{g}_2, \dots, \mathbf{g}_K]$. The channel \mathbf{h}_k is given by

$$\mathbf{h}_k = \mathbf{h}_{d,k} + \mathbf{H}_1 \Theta \mathbf{h}_{2,k}, \quad (3)$$

where $\mathbf{H}_1 \in \mathbb{C}^{M \times N}$ is the LoS deterministic channel between the RIS and the BS (where $h_{1,m,n}$ is the channel between BS antenna m and RIS element n), and $\mathbf{h}_{2,k} \in \mathbb{C}^{N \times 1}$ and $\mathbf{h}_{d,k} \in \mathbb{C}^{M \times 1}$ are the block fading channel vectors between user k and the RIS and user k and the BS respectively. Also $\Theta = \text{diag}(v_1, v_2, \dots, v_N)$ represents the response of the RIS, where $v_n = \alpha_n e^{j\phi_n}$, $\phi_n \in [0, 2\pi]$ is the phase-shift introduced by the element n and $\alpha_n \in [0, 1]$ is the amplitude reflection constant. Note that the LoS assumption for BS-RIS channel matrix is a practical and common assumption in literature [11], [13], [23] given both BS and RIS are generally elevated high with few obstacles around, resulting in a stable LoS channel. The BS utilizes the estimates of \mathbf{h}_k (whose estimation will be discussed in Sec.III), denoted as $\hat{\mathbf{h}}_k$, to implement MRT precoding. MRT is a popular precoding scheme for massive MIMO settings, since it reduces the computational complexity greatly as compared to zero-forcing and regularized zero-forcing precoding, which involve the inversion of the Gram matrix of joint users' channel matrices. With MRT, the precoding vector is given as $\mathbf{g}_k = \zeta \hat{\mathbf{h}}_k$, where ζ satisfies the power constraint in (2) as,

$$\zeta^2 = P_{max} / \Psi, \quad (4)$$

where $\Psi = \mathbb{E} \left[\text{tr} \left(\mathbf{P} \hat{\mathbf{H}} \hat{\mathbf{H}}^H \right) \right]$ and $\hat{\mathbf{H}}^H = [\hat{\mathbf{h}}_1, \hat{\mathbf{h}}_2 \dots \hat{\mathbf{h}}_K] \in \mathbb{C}^{M \times K}$.

B. Channel Models

In this work, we will analyze the SINR and downlink sum-rate performance under the Rician and Rayleigh fading models for $\mathbf{h}_{2,k}$ and $\mathbf{h}_{d,k}$. Under Rician fading, the channels are expressed as

$$\mathbf{h}_{2,k}^{ric} = \mathbf{h}_{2,k}^{NLoS} + \bar{\mathbf{h}}_{2,k}, \quad \mathbf{h}_{d,k}^{ric} = \mathbf{h}_{d,k}^{NLoS} + \bar{\mathbf{h}}_{d,k} \quad (5)$$

where $\mathbf{h}_{2,k}^{NLoS} = \sqrt{\frac{1}{\kappa_{2,k}+1}} \mathbf{h}_{2,k}^{ray}$, $\mathbf{h}_{2,k}^{ray} \sim \mathcal{CN}(0, \beta_{2,k} \mathbf{I}_N)$ and $\mathbf{h}_{d,k}^{NLoS} = \sqrt{\frac{1}{\kappa_{d,k}+1}} \mathbf{h}_{d,k}^{ray}$, $\mathbf{h}_{d,k}^{ray} \sim \mathcal{CN}(0, \beta_{d,k} \mathbf{I}_N)$ are the NLoS channel components. The LoS components, $\bar{\mathbf{h}}_{2,k}$ and $\bar{\mathbf{h}}_{d,k}$ can be modeled as follows [26]:

$$\bar{\mathbf{h}}_{2,k} = \sqrt{\frac{\beta_{2,k} \kappa_{2,k}}{\kappa_{2,k} + 1}} [1, e^{j2\pi d_{h1} \sin(\phi_{d,k})}, \dots, e^{j2\pi d_{h1} (N-1) \sin(\phi_{d,k})}], \quad (6)$$

$$\bar{\mathbf{h}}_{d,k} = \sqrt{\frac{\beta_{d,k} \kappa_{d,k}}{\kappa_{d,k} + 1}} [1, e^{j2\pi d_{h2} \sin(\phi_{2,k})}, \dots, e^{j2\pi d_{h2} (M-1) \sin(\phi_{2,k})}], \quad (7)$$

where d_{h1} and d_{h2} are the BS antenna spacing parameter and RIS element spacing parameter, respectively, $\phi_{d,k}$ and $\phi_{2,k}$ are the angles of arrival (AoA) at user k for the BS-user and RIS-user channels, respectively, $\beta_{i,k}$, $i \in \{2, d\}$ models the large scale fading which includes both the distance dependant pathloss and shadowing, and $\kappa_{i,k}$, $i \in \{2, d\}$ is the Rician factor. Note that the channel attenuation coefficient of the BS to RIS link is captured in the LoS channel \mathbf{H}_1 and is represented by β_1 , where $[\mathbf{H}_1]_{m,n} = \sqrt{\beta_1} e^{j\frac{2\pi}{\lambda}(m-1)d_{h1} \sin \theta_{AP,m} \sin \phi_{AP,m} + (n-1)d_{h2} \sin \theta_{RIS,n} \sin \phi_{RIS,n}}$ with $\theta_{AP,m}$ and $\phi_{AP,m}$ denoting the elevation and azimuth angles of departure (AoD) at the BS, respectively, and $\theta_{RIS,n}$ and $\phi_{RIS,n}$ denoting the elevation and azimuth angles of arrival (AoA) at the RIS, respectively. Under Rician fading, the channels are distributed as

$$\mathbf{h}_{2,k}^{ric} \sim \mathcal{CN}\left(\bar{\mathbf{h}}_{2,k}, \frac{\beta_{2,k}}{\kappa_{2,k} + 1} \mathbf{I}_N\right), \quad \mathbf{h}_{d,k}^{ric} \sim \mathcal{CN}\left(\bar{\mathbf{h}}_{d,k}, \frac{\beta_{d,k}}{\kappa_{d,k} + 1} \mathbf{I}_M\right). \quad (8)$$

The overall channel between user k and the BS, i.e.,

$$\mathbf{h}_k^{ric} = \mathbf{h}_{d,k}^{NLoS} + \bar{\mathbf{h}}_{d,k} + \mathbf{H}_1 \Theta \mathbf{h}_{2,k}^{NLoS} + \mathbf{H}_1 \Theta \bar{\mathbf{h}}_{2,k} \quad (9)$$

can be statistically represented as

$$\mathbf{h}_k^{ric} = \bar{\mathbf{h}}_{d,k} + \mathbf{H}_1 \Theta \bar{\mathbf{h}}_{2,k} + \mathbf{A}_k^{ric^{1/2}} \mathbf{z}_k, \quad (10)$$

where $\mathbf{z}_k \sim \mathcal{CN}(\mathbf{0}, \mathbf{I}_M)$ and $\mathbf{A}_k^{ric} = \frac{\beta_{d,k}}{\kappa_{d,k} + 1} \mathbf{I}_M + \frac{\beta_{2,k}}{\kappa_{2,k} + 1} \mathbf{H}_1 \Theta \Theta^H \mathbf{H}_1^H$.

Note that $\Theta \Theta^H = \text{diag}(\boldsymbol{\alpha})$, where $\boldsymbol{\alpha} = [\alpha_1^2, \dots, \alpha_N^2]$. The result in (9) can be obtained by noting that \mathbf{h}_k^{ric} is a sum of two deterministic vectors which determine the mean $\bar{\mathbf{h}}_{d,k} + \mathbf{H}_1 \Theta \bar{\mathbf{h}}_{2,k}$ of \mathbf{h}_k^{ric} , and a sum of two independent Gaussian vectors of zero mean resulting in the correlation matrix \mathbf{A}_k^{ric} .

The Rayleigh fading channel models $\mathbf{h}_{d,k}^{ray}$ and $\mathbf{h}_{2,k}^{ray}$ are already defined in $\mathbf{h}_{2,k}^{NLoS}$ and $\mathbf{h}_{d,k}^{NLoS}$, and can be retrieved by setting $\kappa_{d,k}$ and $\kappa_{2,k}$ as 0 in (5). The statistical representation of \mathbf{h}_k^{ray} can also be obtained by setting the Rician factors as 0 in (10). In this work we aim at deriving the asymptotic deterministic equivalent of the ergodic achievable sum-rate under imperfect CSI and MRT precoding for both Rayleigh and Rician fading channels. Additionally, we optimize the RIS configuration using a gradient ascent algorithm to maximize the sum-rate performance.

III. CHANNEL ESTIMATION PROTOCOLS

In this section, we propose two channel estimation protocols under the time-division duplexing (TDD) strategy, where the BS exploits channel reciprocity to estimate the downlink channels. The channel coherence period of τ sec is divided into an uplink training phase of τ_u sec and a downlink transmission phase of τ_d sec. Throughout the training phase, the users transmit mutually orthogonal pilot sequences.

A. MMSE-ON/OFF Protocol

Optimizing RIS in the data transmission phase, requires estimates of $\mathbf{h}_{d,k}$, \mathbf{H}_1 , and $\mathbf{h}_{2,k}$. Since the RIS cannot perform channel estimation on its own, so the BS has to estimate all the channels and share the required RIS configuration with the RIS controller. One way to obtain all this CSI is the least square (LS)-ON/OFF protocol proposed in [18] for a single-user system.¹ We extend this to the multi-user system under MMSE estimation, which is well-known to achieve a lower mean squared error (MSE) than LS. To this end, note that we can write

$$\mathbf{H}_1 \mathbf{O} \mathbf{h}_{2,k} = \mathbf{H}_{0,k} \mathbf{v}, \quad (11)$$

where $\mathbf{H}_{0,k} = \mathbf{H}_1 \text{diag}(\mathbf{h}_{2,k}^T)$ and $\mathbf{v} = [v_1, v_2, \dots, v_N]^T \in \mathbb{C}^{N \times 1}$. With this representation, we have cascaded \mathbf{H}_1 and $\mathbf{h}_{2,k}$ as $\mathbf{H}_{0,k} \in \mathbb{C}^{M \times N}$, where $\mathbf{H}_{0,k} = [\mathbf{h}_{0,k,1}, \dots, \mathbf{h}_{0,k,N}]$ is a matrix of N column vectors, given by $\mathbf{h}_{0,k,i} = \mathbf{h}_{1,i} h_{2,k,i}$ with $h_{2,k,i}$ as the i 'th element of vector $\mathbf{h}_{2,k}$ and $\mathbf{h}_{1,i}$ as the i 'th column of \mathbf{H}_1 . Each vector $\mathbf{h}_{0,k,i} \in \mathbb{C}^{M \times 1}$ (shown in red curved arrows in Fig. 1) can be interpreted as the channel from the user to the BS through the element i of the RIS only, which can similarly be expressed as a sum of NLoS and LoS components, i.e., $\mathbf{h}_{0,k,i} = \mathbf{h}_{0,k,i}^{NLoS} + \bar{\mathbf{h}}_{0,k,i}$, where $\mathbf{h}_{0,k,i}^{NLoS} = \mathbf{h}_{1,i} h_{2,k,i}^{NLoS}$ and $\bar{\mathbf{h}}_{0,k,i} = \mathbf{h}_{1,i} \bar{h}_{2,k,i}$. We will focus on the MMSE estimation of $\mathbf{h}_{0,k,i}$, $i = 1, \dots, N$ and $\mathbf{h}_{d,k}$ for $k = 1, \dots, K$ at the BS. Correlating the received training signal at the BS with the pilot signal of user k , the BS obtains the received observation

$$\mathbf{r}_k^{tr} = (\mathbf{h}_{d,k} + \sum_{i=1}^N \mathbf{h}_{0,k,i} v_i) + \mathbf{n}_k^{tr}, \quad k = 1, \dots, K, \quad (12)$$

where $\mathbf{n}_k^{tr} \sim \mathcal{CN}(\mathbf{0}, \frac{1}{\rho_{tr}} \mathbf{I}_M)$ is the received noise in the uplink and $\rho_{tr} > 0$ is the effective training SNR.

To enable the estimation of $\mathbf{h}_{d,k}$ and $\mathbf{h}_{0,k,i}$, $\forall i$, at the BS while keeping the RIS passive, the channel estimation interval is divided into $N + 1$ sub-phases of length $\tau_s = \frac{\tau_u}{N+1}$. The RIS reflecting elements are controlled such that during the first sub-interval, all RIS elements are turned OFF, i.e. $\alpha_n = 0$, $\forall n$. Therefore in this sub-phase the BS will only receive the pilot signals transmitted over $\mathbf{h}_{d,k}$ which it can then estimate. In the following N sub-phases, i.e., sub-phases $i + 1$ with $i = 1, \dots, N$, only the i^{th} RIS element is turned ON in the full reflection mode (i.e. $\alpha_i = 1$, $\phi_i = 0$), while the others are kept OFF to enable the estimation of $\mathbf{h}_{0,k,i}$.

We discuss the estimation under Rician channel below, and provide the estimates under

¹The asymptotic analysis can also be extended under other channel estimation protocols, like the one in [19].

Rayleigh channel case in Corollary 1. Under Rician fading, the received observation vector in the first sub-phase of the channel estimation phase is given as,

$$\mathbf{r}_{1,k}^{tr} = \mathbf{h}_{d,k}^{NLoS} + \bar{\mathbf{h}}_{d,k} + \mathbf{n}_{1,k}^{tr}, \quad k = 1, \dots, K. \quad (13)$$

The BS estimates $\mathbf{h}_{d,k}^{NLoS}$ from $\mathbf{r}_{1,k}^{tr}$ using MMSE estimation, to obtain $\hat{\mathbf{h}}_{d,k}^{NLoS} = \mathbf{h}_{d,k}^{NLoS} + \tilde{\mathbf{h}}_{d,k}^{NLoS}$ where $\tilde{\mathbf{h}}_{d,k}^{NLoS}$ is the channel estimation error. The received observation vector during sub-phase $(i + 1)$ is given as,

$$\mathbf{r}_{i+1,k}^{tr} = \mathbf{h}_{d,k}^{NLoS} + \bar{\mathbf{h}}_{d,k} + \mathbf{h}_{0,k,i}^{NLoS} + \bar{\mathbf{h}}_{0,k,i} + \mathbf{n}_{i,k}^{tr}, \quad k = 1, \dots, K, \quad i = 1, \dots, N. \quad (14)$$

Since the BS already has $\hat{\mathbf{h}}_{d,k}^{NLoS}$ at the end of first sub-phase, it subtracts it from the subsequent observation vectors in (14) and obtain,

$$\tilde{\mathbf{r}}_{i+1,k}^{tr} = \tilde{\mathbf{h}}_{d,k}^{NLoS} + \bar{\mathbf{h}}_{d,k} + \mathbf{h}_{0,k,i}^{NLoS} + \bar{\mathbf{h}}_{0,k,i} + \mathbf{n}_{i,k}^{tr}, \quad (15)$$

from which the BS estimates $\mathbf{h}_{0,k,i}^{NLoS}$ to obtain $\hat{\mathbf{h}}_{0,k,i}^{NLoS} = \mathbf{h}_{0,k,i}^{NLoS} + \tilde{\mathbf{h}}_{0,k,i}^{NLoS}$ where $\tilde{\mathbf{h}}_{0,k,i}^{NLoS}$ is the error. The resulting MMSE estimate for $\mathbf{h}_k^{ric} = \mathbf{h}_{d,k}^{ric} + \sum_{i=1}^N \mathbf{h}_{0,k,i}^{ric} v_i$ is given in the following lemma.

Lemma 1: The MMSE estimate of \mathbf{h}_k^{ric} (9) under the Rician channel model in (5) and the ON/OFF protocol is given as

$$\hat{\mathbf{h}}_k^{ric} = \hat{\mathbf{h}}_{d,k}^{NLoS} + \bar{\mathbf{h}}_{d,k} + \sum_{i=1}^N \hat{\mathbf{h}}_{0,k,i}^{NLoS} v_i + \sum_{i=1}^N \bar{\mathbf{h}}_{0,k,i} v_i, \quad (16)$$

where the MMSE estimates of $\mathbf{h}_{d,k}^{NLoS}$ and $\mathbf{h}_{0,k,i}^{NLoS}$ are given by

$$\hat{\mathbf{h}}_{d,k}^{NLoS} = \frac{\beta_{d,k}^{NLoS}}{\beta_{d,k}^{NLoS} + \frac{1}{\rho_{tr}}} (\mathbf{r}_{1,k}^{tr} - \bar{\mathbf{h}}_{d,k}), \quad (17)$$

$$\hat{\mathbf{h}}_{0,k,i}^{NLoS} = \mathbf{R}_{0,i,k}^{NLoS} \mathbf{Q}_{i,k}^{NLoS} (\tilde{\mathbf{r}}_{i+1,k}^{tr} - \bar{\mathbf{h}}_{d,k} - \bar{\mathbf{h}}_{0,k,i}), \quad (18)$$

with $\mathbf{r}_{1,k}^{tr}$ and $\tilde{\mathbf{r}}_{i+1,k}^{tr}$ as defined in (13) and (15), $\beta_{i,k}^{NLoS} = \frac{\beta_{i,k}}{\kappa_{i,k} + 1}$ $i \in \{d, 2\}$, $\mathbf{R}_{0,i,k}^{NLoS} = \beta_{2,k}^{NLoS} \mathbf{h}_{1,i} \mathbf{h}_{1,i}^H$, $\mathbf{Q}_{i,k}^{NLoS} = \left(\mathbf{C}_{\tilde{\mathbf{h}}_{d,k}^{NLoS} \tilde{\mathbf{h}}_{d,k}^{NLoS} H} + \beta_{2,k}^{NLoS} \mathbf{h}_{1,i} \mathbf{h}_{1,i}^H + \frac{1}{\rho_{tr}} \mathbf{I}_M \right)^{-1}$ and $\mathbf{C}_{\tilde{\mathbf{h}}_{d,k}^{NLoS} \tilde{\mathbf{h}}_{d,k}^{NLoS} H} = \frac{\beta_{d,k}^{NLoS}}{\rho_{tr} \beta_{d,k}^{NLoS} + 1} \mathbf{I}_M$.

Proof: The proof is provided in Appendix A. ■

Note that both $\hat{\mathbf{h}}_{d,k}^{NLoS}$ and $\hat{\mathbf{h}}_{0,k,i}^{NLoS}$ follow Gaussian distribution. Also under the orthogonality property of the MMSE estimates, the estimation error $\tilde{\mathbf{h}}_{d,k}^{NLoS}$, follows a Gaussian distribution and is uncorrelated with $\hat{\mathbf{h}}_{d,k}^{NLoS}$ (as well as independent due to joint Gaussianity). A similar discussion applies to the error vector $\tilde{\mathbf{h}}_{0,k,i}^{NLoS}$.

Using these results, $\hat{\mathbf{h}}_k^{ric}$ is statistically equivalent to a correlated Rician channel as follows.

Theorem 1: The channel estimate $\hat{\mathbf{h}}_k^{ric} = \hat{\mathbf{h}}_{d,k}^{NLoS} + \bar{\mathbf{h}}_{d,k} + \sum_{i=1}^N \hat{\mathbf{h}}_{0,k,i}^{NLoS} v_i + \sum_{i=1}^N \bar{\mathbf{h}}_{0,k,i} v_i$ can be

represented as,

$$\hat{\mathbf{h}}_k^{ric} = \bar{\mathbf{h}}_{d,k} + \sum_{i=1}^N \bar{\mathbf{h}}_{0,k,i} v_i + \mathbf{C}_k^{ric^{1/2}} \mathbf{q}_k, \quad (19)$$

where $\mathbf{q}_k \sim \mathcal{CN}(0, \mathbf{I}_M)$ and,

$$\begin{aligned} \mathbf{C}_k^{ric} &= \frac{\beta_{d,k}^{NLoS^2}}{\beta_{d,k}^{NLoS} + \frac{1}{\rho_{tr}}} \mathbf{I}_M + \sum_{i=1}^N \mathbf{R}_{0,i,k}^{NLoS} \mathbf{Q}_{i,k}^{NLoS} \left(\beta_{2,k}^{NLoS} \mathbf{h}_{1,i} \mathbf{h}_{1,i}^H + \frac{1}{\rho_{tr}} \mathbf{I}_M \right) \mathbf{Q}_{i,k}^{NLoS^H} \mathbf{R}_{0,i,k}^{NLoS^H} \\ &+ \sum_{i=1}^N \sum_{j=1}^N v_i \mathbf{R}_{0,i,k}^{NLoS} \mathbf{Q}_{i,k}^{NLoS} \mathbf{C}_{\bar{\mathbf{h}}_{d,k}^{NLoS} \bar{\mathbf{h}}_{d,k}^{NLoS^H}} \mathbf{Q}_{j,k}^{NLoS^H} \mathbf{R}_{0,j,k}^{NLoS^H} v_j^*. \end{aligned} \quad (20)$$

Proof: The proof is provided in Appendix B. ■

For Rayleigh fading, the following corollary can be obtained from Theorem 1.

Corollary 1: The MMSE estimate of \mathbf{h}_k^{ray} under Rayleigh fading $\mathbf{h}_{d,k}$ and $\mathbf{h}_{2,k}$ is given as

$$\hat{\mathbf{h}}_k^{ray} = \hat{\mathbf{h}}_{d,k}^{ray} + \sum_{i=1}^N \hat{\mathbf{h}}_{0,k,i}^{ray}, \quad (21)$$

where the MMSE estimates of $\mathbf{h}_{d,k}^{ray}$ and $\mathbf{h}_{0,k,i}^{ray}$ are

$$\hat{\mathbf{h}}_{d,k}^{ray} = \frac{\beta_{d,k}}{\beta_{d,k} + \frac{1}{\rho_{tr}}} \mathbf{r}_{1,k}^{tr}, \quad (22)$$

$$\hat{\mathbf{h}}_{0,k,i}^{ray} = \mathbf{R}_{0,i,k}^{ray} \mathbf{Q}_{i,k}^{ray} \tilde{\mathbf{r}}_{i+1,k}^{tr}, \quad (23)$$

$$\begin{aligned} \mathbf{r}_{1,k}^{tr} &= \mathbf{h}_{d,k}^{ray} + \mathbf{n}_{1,k}^{tr}, \quad \tilde{\mathbf{r}}_{i+1,k}^{tr} = \tilde{\mathbf{h}}_{d,k}^{ray} + \mathbf{h}_{0,k,i}^{ray} + \mathbf{n}_{i,k}^{tr}, \quad \tilde{\mathbf{h}}_{d,k}^{ray} = \mathbf{h}_{d,k}^{ray} - \hat{\mathbf{h}}_{d,k}^{ray}, \quad \mathbf{R}_{0,i,k}^{ray} = \beta_{2,k} \mathbf{h}_{1,i} \mathbf{h}_{1,i}^H, \\ \mathbf{Q}_{i,k}^{ray} &= \left(\mathbf{C}_{\tilde{\mathbf{h}}_{d,k}^{ray} \tilde{\mathbf{h}}_{d,k}^{ray^H}} + \beta_{2,k} \mathbf{h}_{1,i} \mathbf{h}_{1,i}^H + \frac{1}{\rho_{tr}} \mathbf{I}_M \right)^{-1} \quad \text{and} \quad \mathbf{C}_{\tilde{\mathbf{h}}_{d,k}^{ray} \tilde{\mathbf{h}}_{d,k}^{ray^H}} = \frac{\beta_{d,k}}{\rho_{tr} \beta_{d,k} + 1} \mathbf{I}_M. \end{aligned}$$

The channel estimate $\hat{\mathbf{h}}_k^{ray} = \hat{\mathbf{h}}_{d,k}^{ray} + \sum_{i=1}^N \hat{\mathbf{h}}_{0,k,i}^{ray} v_i$ is statistically equivalent to

$$\hat{\mathbf{h}}_k^{ray} = \mathbf{C}_k^{ray^{1/2}} \mathbf{q}_k, \quad (24)$$

where $\mathbf{q}_k \sim \mathcal{CN}(0, \mathbf{I}_M)$ and,

$$\begin{aligned} \mathbf{C}_k^{ray} &= \frac{\beta_{d,k}^2}{\beta_{d,k} + \frac{1}{\rho_{tr}}} \mathbf{I}_M + \sum_{i=1}^N \mathbf{R}_{0,i,k}^{ray} \mathbf{Q}_{i,k}^{ray} \left(\beta_{2,k} \mathbf{h}_{1,i} \mathbf{h}_{1,i}^H + \frac{1}{\rho_{tr}} \mathbf{I}_M \right) \mathbf{Q}_{i,k}^{ray^H} \mathbf{R}_{0,i,k}^{ray^H} \\ &+ \sum_{i=1}^N \sum_{j=1}^N v_i \mathbf{R}_{0,i,k}^{ray} \mathbf{Q}_{i,k}^{ray} \mathbf{C}_{\tilde{\mathbf{h}}_{d,k}^{ray} \tilde{\mathbf{h}}_{d,k}^{ray^H}} \mathbf{Q}_{j,k}^{ray^H} \mathbf{R}_{0,j,k}^{ray^H} v_j^*. \end{aligned} \quad (25)$$

Remark 1: The channel estimate $\hat{\mathbf{h}}_k^{ray}$ in (24) shows that under Rayleigh fading, the RIS phase-shifts only appear in term $\sum_{i=1}^N \sum_{j=1}^N v_i \mathbf{R}_{0,i,k}^{ray} \mathbf{Q}_{i,k}^{ray} \mathbf{C}_{\tilde{\mathbf{h}}_{d,k}^{ray} \tilde{\mathbf{h}}_{d,k}^{ray^H}} \mathbf{Q}_{j,k}^{ray^H} \mathbf{R}_{0,j,k}^{ray^H} v_j^*$, which is related to the channel estimation error $\tilde{\mathbf{h}}_{d,k}^{ray}$ in the direct channel. In the Rician fading case, the channel estimate $\hat{\mathbf{h}}_k^{ric}$ in (19) shows that the RIS-phase shifts also appear in the LoS terms, i.e., $\sum_{i=1}^N \bar{\mathbf{h}}_{0,k,i} v_i$. This shows the impact of RIS phase-shifts under both fading environments and the importance of optimizing the phase-shifts especially under the Rician case.

B. MMSE-Direct Estimation

In the DE scheme, instead of estimating the individual channels $\mathbf{h}_{d,k}$ and $\mathbf{h}_{0,k,i}$ s, the BS directly estimates the overall channel \mathbf{h}_k for each user for a given RIS reflect beamforming vector \mathbf{v} (or equivalently RIS reflect beamforming matrix Θ). This is done in a single sub-phase of length $\tau_s = \tau_u$ sec, using the training signal in (12). The impact of the choice of \mathbf{v} during channel estimation on the sum-rate performance will be studied in Sec. IV in the large system limit. The MMSE estimate of \mathbf{h}_k , for any given \mathbf{v} , is now stated for both fading models.

Lemma 2: The MMSE estimate of \mathbf{h}_k^{ric} (9) under the Rician channel model in (5) and the DE protocol is given as

$$\hat{\mathbf{h}}_k^{ric} = \bar{\mathbf{h}}_{d,k} + \mathbf{H}_1 \Theta \bar{\mathbf{h}}_{2,k} + \mathbf{R}_k^{ric} \mathbf{Q}_k^{ric} (\mathbf{y}_k^{tr} - \bar{\mathbf{h}}_{d,k} - \mathbf{H}_1 \Theta \bar{\mathbf{h}}_{2,k}), \quad (26)$$

where $\mathbf{y}_k^{tr} = \mathbf{h}_{d,k}^{ric} + \mathbf{H}_1 \Theta \mathbf{h}_{2,k}^{ric} + \mathbf{n}_k^{tr}$, $\mathbf{Q}_k^{ric} = \left(\beta_{d,k}^{NLoS} \mathbf{I}_M + \beta_{2,k}^{NLoS} \mathbf{H}_1 \text{diag}(\boldsymbol{\alpha}) \mathbf{H}_1^H + \frac{\mathbf{I}_M}{\rho_{tr}} \right)^{-1}$, and $\mathbf{R}_k^{ric} = \beta_{d,k}^{NLoS} \mathbf{I}_M + \beta_{2,k}^{NLoS} \mathbf{H}_1 \text{diag}(\boldsymbol{\alpha}) \mathbf{H}_1^H$.

Proof: The proof uses the fact that $\Theta \Theta^H = \text{diag}(\boldsymbol{\alpha})$, since $|v_n|^2 = |\alpha_n \exp(j\phi_n)|^2 = \alpha_n^2$. ■

The following then follows for the Rayleigh fading channel.

Corollary 2: The MMSE estimate of the overall channel $\mathbf{h}_k^{ray} = \mathbf{h}_{d,k}^{ray} + \mathbf{H}_1 \Theta \mathbf{h}_{2,k}^{ray}$, denoted as $\hat{\mathbf{h}}_k^{ray}$, under DE and Rayleigh fading is given as

$$\hat{\mathbf{h}}_k^{ray} = \mathbf{R}_k^{ray} \mathbf{Q}_k^{ray} \mathbf{y}_k^{tr}, \quad (27)$$

where $\mathbf{R}_k^{ray} = \beta_{d,k} \mathbf{I}_M + \beta_{2,k} \mathbf{H}_1 \text{diag}(\boldsymbol{\alpha}) \mathbf{H}_1^H$, $\mathbf{Q}_k^{ray} = \left(\beta_{d,k} \mathbf{I}_M + \beta_{2,k} \mathbf{H}_1 \text{diag}(\boldsymbol{\alpha}) \mathbf{H}_1^H + \frac{\mathbf{I}_M}{\rho_{tr}} \right)^{-1}$, and $\mathbf{y}_k^{tr} = \mathbf{h}_{d,k}^{ray} + \mathbf{H}_1 \Theta \mathbf{h}_{2,k}^{ray} + \mathbf{n}_k^{tr}$.

The DE scheme reduces the number of channel estimation sub-phases from $N + 1$ to a single subphase, and therefore significantly reduces the estimation complexity and pilot overhead. The downside to this protocol is that although the estimates in (26) and (27) can be used to implement the precoding at the BS, they can not be used to design the RIS phases based on the exact sum-rate expression defined later in (30), which will require the estimates $\hat{\mathbf{h}}_{d,k}$ and $\hat{\mathbf{h}}_{0,k,i}$. However, if the RIS phases can be chosen using knowledge of only the channel statistics as will be the case in the next section which focuses on large systems, then DE is a very desirable scheme. This is because CSI will only be needed for implementing MRT precoding, for which the BS can use (26) and (27) instead of (16) and (21), while the RIS phases will be tuned for the given channel statistics instead of a specific channel state.

IV. ASYMPTOTIC ANALYSIS

In this section we derive the deterministic equivalents of users' SINRs and ergodic rates. We exploit the channel hardening property in large-scale MIMO systems using a technique from [27], which is widely applied to large-scale MIMO systems [24], [25]. The main idea is to decompose y_k in (1) using the definition of \mathbf{x} as $y_k = \sqrt{p_k} \mathbb{E}[\mathbf{h}_k^H \mathbf{g}_k] s_k + \sqrt{p_k} (\mathbf{h}_k^H \mathbf{g}_k - \mathbb{E}[\mathbf{h}_k^H \mathbf{g}_k]) s_k + \sum_{l \neq k} \sqrt{p_l} \mathbf{h}_k^H \mathbf{g}_l s_l + n_k$ and assume that the average effective channel $\mathbb{E}[\mathbf{h}_k^H \mathbf{g}_k]$ is perfectly known at user k . By treating the interference and channel uncertainty as worst-case independent Gaussian noise, we conclude that user k can achieve the rate,

$$R_k = \log_2(1 + \gamma_k), \quad (28)$$

without knowing the instantaneous values of $\mathbf{h}_k^H \mathbf{g}_k$. The parameter γ_k can be interpreted as the effective average downlink SINR of user k and is defined under MRT precoding as,

$$\gamma_k = \frac{p_k |\mathbb{E}[\mathbf{h}_k^H \hat{\mathbf{h}}_k]|^2}{p_k \text{Var}[\mathbf{h}_k^H \hat{\mathbf{h}}_k] + \sum_{l \neq k} p_l \mathbb{E}[|\mathbf{h}_k^H \hat{\mathbf{h}}_l|^2] + \frac{\Psi}{\rho}}, \quad (29)$$

where $\rho = \frac{P_{max}}{\sigma^2}$. The ergodic achievable sum-rate is obtained as

$$R_{sum} = \sum_{k=1}^K \log_2(1 + \gamma_k). \quad (30)$$

We assume $\alpha_n = 1, \forall n$ in the subsequent part of this work. This assumption is justified due to the significant recent advancements made in the design and fabrication of loss-less metasurfaces [28], [29], which has led to most existing works on RIS-assisted systems to make a similar assumption. This section will first motivate the asymptotic analysis, introduce the required RMT tools and then derive the deterministic equivalents.

A. Motivation and Useful Lemmas

The users' ergodic rates, which are important system performance metrics, are generally difficult to study for finite system dimensions. It turns out that in an asymptotic (large system dimension) regime, the users' SINRs and ergodic rates tend to approach deterministic quantities, referred to as deterministic equivalents, which yield useful insights. These equivalents are almost surely (a.s.) tight in the asymptotic limit, i.e. as the system dimensions grow to infinity. They depend only on the statistics of the channel and are very useful to solve important optimization problems in massive MIMO literature [13], [24], [25]. Moreover, these asymptotic approximations turn out to be very accurate for moderate system dimensions as well. Under this motivation, we exploit the statistical distribution of \mathbf{h}_k and large values of M, N, K envisioned for 5G (and

beyond) networks to compute the deterministic approximations of the users' SINRs and ergodic rates under both MMSE-ON/OFF estimation and MMSE-DE protocols.

Before we begin the asymptotic analysis, we formalize the required assumptions below [30].

Assumption 1. M , N and K grow large with a bounded ratio as $0 < \liminf_{M,K \rightarrow \infty} \frac{K}{M} \leq \limsup_{M,K \rightarrow \infty} \frac{K}{M} < \infty$ and $0 < \liminf_{M,N \rightarrow \infty} \frac{M}{N} \leq \limsup_{M,N \rightarrow \infty} \frac{M}{N} < \infty$.

Assumption 2. The LoS channel matrix \mathbf{H}_1 satisfies,

$$\limsup_{M,N \rightarrow \infty} \|\mathbf{H}_1 \mathbf{H}_1^H\| < \infty \quad (31)$$

Assumption 3. The entries of the power matrix $\mathbf{P} = \text{diag}(p_1, p_2, \dots, p_K)$ are of order $O(1/K)$.

The derivations in this section will exploit [25, Lemma 4 (ii), (iii)].

B. Analysis under Rician Fading

We start by presenting the deterministic equivalents for the RIS-assisted channel in (3) under Rician fading, followed by performance optimization.

1) *Deterministic Equivalents:* We present the deterministic equivalent of the SINR defined in (29) in the following theorem for Rician fading channels under MMSE ON/OFF protocol.

Theorem 2: Under Assumptions 1-3, the SINR of user k defined in (29), for the channel in (9) and its estimate in (19) under the MMSE ON/OFF protocol satisfies $\gamma_k^{ric} - \gamma_k^{ric^\circ} \xrightarrow[M,N,K \rightarrow \infty]{a.s.} 0$

where

$$\gamma_k^{ric^\circ} = \frac{\frac{p_k}{K} \left| \text{tr} \left(\mathbf{D}_k + \sum_{i=1}^N \left(v_i \mathbf{C}_{\bar{\mathbf{h}}_{d,k}^{NLoS} \bar{\mathbf{h}}_{d,k}^{NLoS H}} \mathbf{R}_{0,i,k}^{NLoS} \mathbf{Q}_{i,k}^{NLoS} + \mathbf{R}_{0,i,k}^{NLoS} \mathbf{R}_{0,i,k}^{NLoS} \mathbf{Q}_{i,k}^{NLoS} \right) + \frac{\beta_{d,k}^{NLoS^2} \mathbf{I}_M}{\beta_{d,k}^{NLoS} + \frac{1}{\rho_{tr}}} \right) \right|^2}{\sum_{l \neq k} \frac{p_l}{K} \text{tr}((\mathbf{D}_l + \mathbf{C}_l^{ric})(\mathbf{D}_k + \mathbf{A}_k^{ric})) + \frac{p_k}{K} \sum_{k=1}^K \frac{\text{tr}(\mathbf{D}_k + \mathbf{C}_k^{ric})}{\rho}} \quad (32)$$

$\mathbf{D}_k = \bar{\mathbf{h}}_{d,k} \bar{\mathbf{h}}_{d,k}^H + \bar{\mathbf{h}}_{d,k} \sum_{i=1}^N v_i^* \bar{\mathbf{h}}_{0,k,i}^H + \sum_{i=1}^N \bar{\mathbf{h}}_{0,k,i} v_i \bar{\mathbf{h}}_{d,k}^H + \sum_{j=1}^N \sum_{i=1}^N \bar{\mathbf{h}}_{0,k,i} v_i v_j^* \bar{\mathbf{h}}_{0,k,j}^H$, \mathbf{A}_k^{ric} is defined in (9) and \mathbf{C}_l^{ric} is defined in Theorem 1 in (20).

Proof: The proof of Theorem 2 is provided in Appendix C. ■

The deterministic equivalent under DE is now presented.

Theorem 3: Under Assumptions 1-3, the SINR of user k defined in (29) with the channel estimate defined in (26) under the DE protocol, satisfies $\gamma_k - \gamma_k^{ric^\circ} \xrightarrow[M,N,K \rightarrow \infty]{a.s.} 0$, where $\gamma_k^{ric^\circ}$ is given as

$$\gamma_k^{ric^\circ} = \frac{\left| \frac{p_k}{K} \text{tr}(\mathbf{D}_k + \beta_{d,k}^{NLoS} \mathbf{R}_k^{ric} \mathbf{Q}_k^{ric} + \sum_{i=1}^N \mathbf{R}_{0,i,k}^{NLoS} \mathbf{R}_k^{ric} \mathbf{Q}_k^{ric}) \right|^2}{\sum_{l \neq k} \frac{p_l}{K} \text{tr}((\mathbf{D}_l + \mathbf{R}_l^{ric} \mathbf{Q}_l^{ric} \mathbf{R}_l^{ric})(\mathbf{D}_k + \mathbf{R}_k^{ric})) + \sum_{k=1}^K \frac{p_k}{K} \frac{\text{tr}(\mathbf{D}_k + \mathbf{R}_k^{ric} \mathbf{Q}_k^{ric} \mathbf{R}_k^{ric})}{\rho}}, \quad (33)$$

and \mathbf{R}_k^{ric} and \mathbf{Q}_k^{ric} are defined in Lemma 2.

Proof: The proof of Theorem 3 is similar to the proof of Theorem 2 while considering the MMSE channel estimates as defined in Lemma 2. ■

Next, we simplify the result in Theorem 2 for the scenario where perfect CSI is available, which we do here for benchmarking purposes.

Corollary 3: Under the setting of Theorem 2, and assuming perfect CSI, $\gamma_k^{ric^\circ}$ becomes,

$$\gamma_k^{ric^\circ} = \frac{\frac{p_k}{K} |\text{tr}(\mathbf{D}_k + \mathbf{A}_k^{ric})|^2}{\sum_{l \neq k} \text{tr}\left(\frac{p_l}{K} (\mathbf{D}_l + \mathbf{A}_l^{ric})(\mathbf{D}_k + \mathbf{A}_k^{ric})\right) + \frac{p_k}{K} \sum_{k=1}^K \frac{\text{tr}(\mathbf{D}_k + \mathbf{A}_k^{ric})}{\rho}} \quad (34)$$

where \mathbf{A}_k^{ric} is defined in (9).

Proof: The proof follows by letting $\rho_{tr} \rightarrow \infty$ in Theorem 2. ■

It is interesting to note that asymptotically, the RIS reflect beamforming matrix Θ appears in all terms involving the LoS channel components and plays a negligible role in the NLoS terms as shown in (32) and (33). Optimizing the RIS phase shifts is therefore expected to provide reflect beamforming gains under Rician fading in the asymptotic regime.

Next we express the deterministic equivalents of user rates in the following corollary.

Corollary 4: Under Assumptions 1-3, it follows from the continuous mapping theorem that the individual downlink rates R_k^{ric} of the users converge as $R_k^{ric} - R_k^{ric^\circ} \xrightarrow[M, N, K \rightarrow \infty]{a.s.} 0$, where $R_k^{ric^\circ} = \log(1 + \gamma_k^{ric^\circ})$ and $\gamma_k^{ric^\circ}$ is given by (32) or (33) depending on the estimation protocol. An asymptotic approximation for the average sum-rate can be obtained as

$$R_{sum}^{ric^\circ} = \sum_{k=1}^K \log(1 + \gamma_k^{ric^\circ}). \quad (35)$$

2) *Optimization of \mathbf{v} in Theorem 2:* Under the MMSE-ON/OFF channel estimation protocol, the elements of \mathbf{v} (or Θ) appear in the deterministic equivalent in (32) in Theorem 2 in all LoS terms and in terms related to the error in the estimation of $\mathbf{h}_{d,k}^{ric}$ propagated to the estimation of $\mathbf{h}_{0,i,k}^{ric}$, $i = 1, \dots, N$. Under the MMSE-DE protocol, the RIS reflect beamforming vector only appears in LoS terms. We formulate the following optimization problem under both estimation protocols.

$$(PI) \quad \max_{v_1, \dots, v_N} \quad R_{sum}^{ric^\circ} = \sum_{k=1}^K \log(1 + \gamma_k^{ric^\circ}) \quad (36a)$$

$$\text{s.t.} \quad |v_n| = 1, \quad \forall n. \quad (36b)$$

(PI) is a constrained maximization problem that can be solved using projected gradient ascent to increase the objective function by taking iterative steps proportional to the positive gradient, as outlined in Algorithm 1. This is done by iteratively updating the RIS phase-shift vector \mathbf{v}^s

Algorithm 1 Projected Gradient Ascent Algorithm for the RIS Design

- 1: **Initialize:** $\mathbf{v}^1 = \exp(j\pi/2)\mathbf{1}_N$, $R_{sum}^{\circ 1} = f(\mathbf{v}^1)$, $\epsilon > 0$, $s = 1$.
 - 2: **Repeat**
 - 3: $[\mathbf{p}^s]_n = \frac{\partial R_{sum}^{\circ}}{\partial v_n} |_{v_n^s}$, $n = 1, \dots, N$;
 - 4: $\mu = \text{backtrack line search}(f(\mathbf{v}^s), \mathbf{p}^s, \mathbf{v}^s)$ [31];
 - 5: $\tilde{\mathbf{v}}^{s+1} = \mathbf{v}^s + \mu\mathbf{p}^s$; $\mathbf{v}^{s+1} = \exp(j\arg(\tilde{\mathbf{v}}^{s+1}))$;
 - 6: $R_{sum}^{o^{s+1}} = f(\mathbf{v}^{s+1})$;
 - 7: Update $s = s + 1$;
 - 8: **Until** $\|R_{sum}^{o^{s+1}} - R_{sum}^o\|^2 < \epsilon$; Obtain $\mathbf{v}^* = \mathbf{v}^{s+1}$;
-

in a step proportional to the positive gradient, \mathbf{p}^s as $\tilde{\mathbf{v}}^{s+1} = \mathbf{v}^s + \mu\mathbf{p}^s$, where the step size μ is obtained using backtracking line search. The solution $\tilde{\mathbf{v}}^{s+1}$ is projected onto the closest feasible point that satisfies the constraint in (36b). It is important to note, however, that (P1) is a non-convex problem, and a projected gradient ascent algorithm will only provide a local optimum. Thus, we make no claim about the global optimality of the solution. The derivative of $R_{sum}^{ric\circ}$ with respect to v_n , $n = 1, \dots, N$ is stated below under both estimation protocols.

Lemma 3: The derivative of $R_{sum}^{ric\circ}$ defined in (35) for the SINR under MMSE-ON/OFF protocol in (32) with respect to v_n is given as

$$\frac{\partial R_{sum}^{ric\circ}}{\partial v_n} = \sum_{k=1}^K \frac{4d_k \sqrt{\frac{p_k q_k}{K}} \text{tr}(\sum_i v_i \bar{\mathbf{h}}_{0,k,i} \bar{\mathbf{h}}_{0,k,n}^H + \bar{\mathbf{h}}_{0,k,n} \bar{\mathbf{h}}_{d,k}^H + \mathbf{C}_{\tilde{\mathbf{h}}_{d,k}^{NLoS}} \tilde{\mathbf{h}}_{d,k}^{NLoS^H} \mathbf{R}_{0,n,k}^{NLoS} \mathbf{Q}_{n,k}^{NLoS}) - q_k d'_k}{(1 + \gamma_k^o) \ln(2) d_k^2}, \quad (37)$$

where q_k and d_k are the numerator and the denominator of (32), respectively, and

$$\begin{aligned} d'_k &= \sum_{l \neq k} \frac{p_l}{K} \text{tr} \left((\mathbf{D}_k + \mathbf{A}_k^{ric}) \left(2 \sum_{i=1}^N v_i \mathbf{R}_{0,i,l}^{NLoS} \mathbf{Q}_{i,l}^{NLoS} \mathbf{C}_{\tilde{\mathbf{h}}_{d,l}^{NLoS}} \tilde{\mathbf{h}}_{d,l}^{NLoS^H} \mathbf{Q}_{n,l}^{NLoS^H} \mathbf{R}_{0,n,l}^{NLoS^H} \right) \right) \\ &+ \text{tr} \left((\mathbf{D}_k + \mathbf{A}_k^{ric}) \left(2 \sum_i v_i \bar{\mathbf{h}}_{0,l,i} \bar{\mathbf{h}}_{0,l,n}^H + \bar{\mathbf{h}}_{0,k,n} \bar{\mathbf{h}}_{d,l}^H \right) \right) \\ &+ \text{tr} \left((\mathbf{D}_l + \mathbf{C}_l^{ric}) \left(2 \sum_i v_i \bar{\mathbf{h}}_{0,k,i} \bar{\mathbf{h}}_{0,k,n}^H + \bar{\mathbf{h}}_{0,k,n} \bar{\mathbf{h}}_{d,k}^H \right) \right) \\ &+ \sum_{k'=1}^K \frac{p_{k'}}{K \rho} \text{tr} \left(2 \sum_{i=1}^N v_i \mathbf{R}_{0,i,k'}^{NLoS} \mathbf{Q}_{i,k'}^{NLoS} \mathbf{C}_{\tilde{\mathbf{h}}_{d,k'}^{NLoS}} \tilde{\mathbf{h}}_{d,k'}^{NLoS^H} \mathbf{Q}_{n,k'}^{NLoS^H} \mathbf{R}_{0,n,k'}^{NLoS^H} \right) \\ &+ \text{tr} \left(2 \sum_i v_i \bar{\mathbf{h}}_{0,k',i} \bar{\mathbf{h}}_{0,k',n}^H + \bar{\mathbf{h}}_{0,k',n} \bar{\mathbf{h}}_{d,k'}^H \right). \end{aligned} \quad (38)$$

Proof. The proof follows from direct application of complex derivatives in [32, 4.1].

Lemma 4: The derivative of $R_{sum}^{ric^\circ}$ defined in (35) for the SINR under MMSE-DE protocol in (33) with respect to v_n is given as

$$\frac{\partial R_{sum}^{ric^\circ}}{\partial v_n} = \sum_{k=1}^K \frac{2d_k \sqrt{\frac{p_k q_k}{K}} (2\text{tr}(\sum_i v_i \bar{\mathbf{h}}_{0,k,i} \bar{\mathbf{h}}_{0,n,k}^H) + \text{tr}(\bar{\mathbf{h}}_{0,n,k} \bar{\mathbf{h}}_{d,k}^H)) - q_k d'_k}{(1 + \gamma_k^\circ) \ln(2) d_k^2}, \quad (39)$$

where q_k and d_k are the numerator and denominator of (33), respectively, and

$$\begin{aligned} d'_k &= \sum_{l \neq k} \frac{p_l}{K} \text{tr} \left((\mathbf{D}_l + \mathbf{R}_l^{ric} \mathbf{Q}_l^{ric} \mathbf{R}_l^{ric}) (2 \sum_i v_i \bar{\mathbf{h}}_{0,k,i} \bar{\mathbf{h}}_{0,k,n}^H + \bar{\mathbf{h}}_{0,k,n} \bar{\mathbf{h}}_{d,k}^H) \right) \\ &\quad + \text{tr} \left((\mathbf{D}_k + \mathbf{R}_k^{ric}) (2 \sum_i v_i \bar{\mathbf{h}}_{0,l,i} \bar{\mathbf{h}}_{0,l,n}^H + \bar{\mathbf{h}}_{0,l,n} \bar{\mathbf{h}}_{d,l}^H) \right) \\ &\quad + \sum_{k=1}^K \frac{p_k}{K \rho} \text{tr} \left(2 \sum_i v_i \bar{\mathbf{h}}_{0,k,i} \bar{\mathbf{h}}_{0,k,n}^H + \bar{\mathbf{h}}_{0,k,n} \bar{\mathbf{h}}_{d,k}^H \right). \end{aligned} \quad (40)$$

Proof. The poof of Lemma 4 is similar to Lemma 3 and therefore omitted.

Using these derivatives along with Algorithm 1, we can optimize the performance of the system.

Next, we derive similar statements under Rayleigh fading.

C. Analysis under Rayleigh Fading

Now we consider the RIS-assisted channel in (3) under Rayleigh fading.

1) *Deterministic Equivalents:* We first present the deterministic equivalent of the SINR defined in (29) in the following theorem for Rayleigh fading channels under MMSE ON/OFF protocol.

Theorem 4: Under Assumptions 1-3, the SINR of user k defined in (29), for the channel in (3) and its estimate in (24) using the ON/OFF MMSE protocol satisfies $\gamma_k^{ray} - \gamma_k^{ray^\circ} \xrightarrow[M, N, K \rightarrow \infty]{a.s.} 0$ where

$$\gamma_k^{ray^\circ} = \frac{\frac{p_k}{K} \left| \text{tr} \left(\sum_{i=1}^N v_i \mathbf{C}_{\tilde{\mathbf{h}}_{d,k}^{ray} \tilde{\mathbf{h}}_{d,k}^{ray}} \mathbf{R}_{0,i,k}^{ray} \mathbf{Q}_{i,k}^{ray} + \frac{\beta_{d,k}^2}{\beta_{d,k} + \frac{1}{\rho_{tr}}} \mathbf{I}_M + \sum_{i=1}^N \mathbf{R}_{0,i,k}^{ray} \mathbf{R}_{0,i,k}^{ray} \mathbf{Q}_{i,k}^{ray} \right) \right|^2}{\sum_{l \neq k} \frac{p_l}{K} \text{tr}(\mathbf{C}_l^{ray} \mathbf{A}_k^{ray}) + \frac{p_k}{K} \sum_{k=1}^K \frac{\text{tr} \mathbf{C}_k^{ray}}{\rho}} \quad (41)$$

and $\mathbf{A}_k = \beta_{2,k} \mathbf{H}_1 \mathbf{H}_1^H + \beta_{d,k} \mathbf{I}_M$ and \mathbf{C}_l^{ray} is defined in (25).

Proof: The proof of Theorem 4 is very similar to the one in Appendix C for Theorem 2 and has been omitted due to space limitations. ■

Two important insights can be drawn from the expression in (41). First, the phase-shifts applied by the RIS elements, i.e. $v_n = \exp(j\alpha_n)$, do not appear anywhere except for the terms involving the MMSE covariance matrix $\mathbf{C}_{\tilde{\mathbf{h}}_{d,k}^{ray} \tilde{\mathbf{h}}_{d,k}^{ray}}$ of $\mathbf{h}_{d,k}^{ray}$. The error in the estimation of $\mathbf{h}_{d,k}^{ray}$ propagates in the estimation of the subsequent $\mathbf{h}_{0,k,i}^{ray}$ s under the proposed ON/OFF channel estimation protocol as shown in (23). If the direct channel is estimated accurately, the phase-shifts will not matter

asymptotically in an RIS-assisted system and RIS will not yield any reflect beamforming gain under Rayleigh fading channels. This phenomenon is caused by the spatial isotropy that holds upon the RIS-assisted channel, which is insensitive to the beamforming between \mathbf{H}_1 and $\mathbf{h}_{2,k}^{ray}$ under Rayleigh fading $\mathbf{h}_{2,k}^{ray}$.² Second, the RIS can still yield an array gain due to the sum over N terms in the numerator. However, there are also terms with sum over N in the denominator. We will see whether the RIS gain in the desired signal energy is larger than the gain in the interference later in this section.

The deterministic equivalent under DE is now presented.

Theorem 5: Under Assumptions 1-3, the SINR of user k defined in (29) with the channel estimate defined in (27) under DE protocol, satisfies $\gamma_k^{ray} - \gamma_k^{ray^\circ} \xrightarrow[M,N,K \rightarrow \infty]{a.s.} 0$, where

$$\gamma_k^{ray^\circ} = \frac{\frac{p_k}{K} \text{tr}(\mathbf{R}_k^{ray} \mathbf{R}_k^{ray} \mathbf{Q}_k^{ray})^2}{\sum_{l \neq k} \frac{p_l}{K} \text{tr}(\mathbf{R}_k^{ray} \mathbf{R}_l^{ray} \mathbf{Q}_l^{ray} \mathbf{R}_l^{ray}) + \sum_{k=1}^K \frac{\frac{p_k}{K} \text{tr}(\mathbf{R}_k^{ray} \mathbf{R}_k^{ray} \mathbf{Q}_k^{ray})}{\rho}}, \quad (42)$$

and \mathbf{R}_k^{ray} and \mathbf{Q}_k^{ray} are defined in Corollary 2.

Proof: The proof of Theorem 5 is similar to Theorem 4 while considering the MMSE expression in (27). ■

Under DE and Rayleigh fading RIS-to-user channels, we see through the expression in (42) that the values of RIS phase-shifts ϕ_n 's do not affect the SINR asymptotically. Therefore for large systems under the DE protocol, the RIS can adopt any values for the phase-shifts during channel estimation as well as during downlink transmission without affecting the sum-rate. However, the RIS will still yield an array gain, which will be explicitly studied later in this section.

Next we simplify the result in Theorem 4 and Theorem 5 for the scenario where perfect CSI is available at the BS for benchmarking purposes. The result is provided in the following Corollary.

Corollary 5: Under the setting of Theorem 4 and under perfect CSI, we have

$$\gamma_k^{ray^\circ} = \frac{\frac{p_k}{K} |\text{tr}(\mathbf{A}_k^{ray})|^2}{\sum_{l \neq k} \text{tr}(\frac{p_l}{K} \mathbf{A}_l^{ray} \mathbf{A}_k^{ray}) + \frac{\frac{p_k}{K} \sum_{k=1}^K \text{tr}(\mathbf{A}_k^{ray})}{\rho}} \quad (43)$$

where $\mathbf{A}_k^{ray} = \beta_{d,k} \mathbf{I}_M + \beta_{2,k} \mathbf{H}_1 \mathbf{H}_1^H$.

Proof: The proof follows by letting $\rho_{tr} \rightarrow \infty$ in Theorem 4 and 5. ■

Next we express the deterministic equivalents of user rates in the following corollary.

Corollary 6: Under Assumptions 1-3, it follows from the continuous mapping theorem that the individual downlink rates R_k^{ray} of the users converge as $R_k^{ray} - R_k^{ray^\circ} \xrightarrow[M,N,K \rightarrow \infty]{a.s.} 0$, where

²The same conclusion holds if both \mathbf{H}_1 and $\mathbf{h}_{2,k}^{ray}$ undergo Rayleigh fading.

$R_k^{ray^\circ} = \log(1 + \gamma_k^{ray^\circ})$ and $\gamma_k^{ray^\circ}$ is given by (41) or (42) depending on the estimation protocol.

An approximation for the average sum-rate can be obtained as

$$R_{sum}^{ray^\circ} = \sum_{k=1}^K \log(1 + \gamma_k^{ray^\circ}). \quad (44)$$

2) *Optimization of \mathbf{v} in Theorem 4:* We have already seen that the values of the phase-shifts applied by the RIS elements do not matter in Rayleigh fading environments under perfect CSI. Under MMSE-ON/OFF estimation protocol, the elements of \mathbf{v} do appear in the deterministic equivalent of the SINR in (41) in Theorem 4 in the terms related to the error in the estimation of $\mathbf{h}_{d,k}^{ray}$ propagated to the estimation of $\mathbf{h}_{0,k,i}^{ray}$. Therefore, under the MMSE-ON/OFF protocol we solve an optimization problem similar to (PI) for Rayleigh fading environments. The problem is again solved using projected gradient ascent (Algorithm 1) and the derivative of $R_{sum}^{ray^\circ}$ for the SINR in (41) with respect to v_n , $n = 1, \dots, N$ is stated below.

Lemma 5: The derivative of $R_{sum}^{ray^\circ}$ defined in (44) with respect to v_n is given as

$$\frac{\partial R_{sum}^{ray^\circ}}{\partial v_n} = \sum_{k=1}^K \frac{2d_k \sqrt{\frac{p_k q_k}{K}} \text{tr}(\mathbf{C}_{\tilde{\mathbf{h}}_{d,k}^{ray} \tilde{\mathbf{h}}_{d,k}^{rayH}} \mathbf{R}_{0,n,k}^{ray} \mathbf{Q}_{n,k}^{ray}) - q_k d_k'}{(1 + \gamma_k^\circ) \ln(2) d_k^2}, \quad (45)$$

where q_k and d_k are the numerator and denominator of (41), respectively, and

$$d_k' = 2 \sum_{i=1}^N v_i \left(\sum_{l \neq k} \frac{p_l}{K} \text{tr}(\mathbf{R}_{0,i,l}^{ray} \mathbf{Q}_{i,l}^{ray} \mathbf{C}_{\tilde{\mathbf{h}}_{d,l}^{ray} \tilde{\mathbf{h}}_{d,l}^{rayH}} \mathbf{Q}_{n,l}^{rayH} \mathbf{R}_{0,n,l}^{rayH} \mathbf{A}_k^{ray}) + \sum_{k=1}^K \frac{p_k}{K \rho} \text{tr}(\mathbf{R}_{0,i,k}^{ray} \mathbf{Q}_{i,k}^{ray} \mathbf{C}_{\tilde{\mathbf{h}}_{d,k}^{ray} \tilde{\mathbf{h}}_{d,k}^{rayH}} \mathbf{Q}_{n,k}^{rayH} \mathbf{R}_{0,n,k}^{rayH}) \right). \quad (46)$$

Proof. The proof follows from direct application of complex derivatives in [32, 4.1].

As one might expect, optimizing the RIS phase-shifts provides a very small gain in the sum-rate performance under Rayleigh fading as will be seen in the simulations since the phase-shifts appear only in terms involving the error covariance matrix $\mathbf{C}_{\tilde{\mathbf{h}}_{d,k}^{ray} \tilde{\mathbf{h}}_{d,k}^{rayH}}$, which are almost negligible.

3) *How Useful is the RIS under Rayleigh Fading?:* To gain explicit insights into the impact of RIS, we consider a special case which assumes $\mathbf{H}_1 = \sqrt{\beta_1} \mathbf{N} \mathbf{U}$, where $\mathbf{U} \in \mathbb{C}^{M \times N}$ is composed of $M \leq N$ leading rows of an arbitrary $N \times N$ unitary matrix [25]. Since in practice each diagonal entry of $\mathbf{H}_1 \mathbf{H}_1^H$ is the sum of N exponential terms of unit norm, so we have normalized \mathbf{U} by \sqrt{N} . Moreover N is assumed to be large but fixed to ensure a bounded spectral norm. The model implies that \mathbf{H}_1 has orthogonal rows. Such a LoS scenario can be realized in practice through proper placement of the RIS array with respect to the BS array as discussed in [33]. This special case will act as an upper-bound on the RIS performance under arbitrary \mathbf{H}_1 . Moreover, we let $\beta_1 \beta_{2,k} = c \beta_{d,k}$, $\forall k$, which is justified in scenarios where RIS is located very close to the

BS. For this special case, the performance of the RIS-assisted system under perfect CSI is given in a compact closed-form as follows.

Corollary 7: For this special case, $\gamma_k^{ray^\circ}$ in Corollary 5 under $p_k = \frac{1}{K}$, $\forall k$ is given as

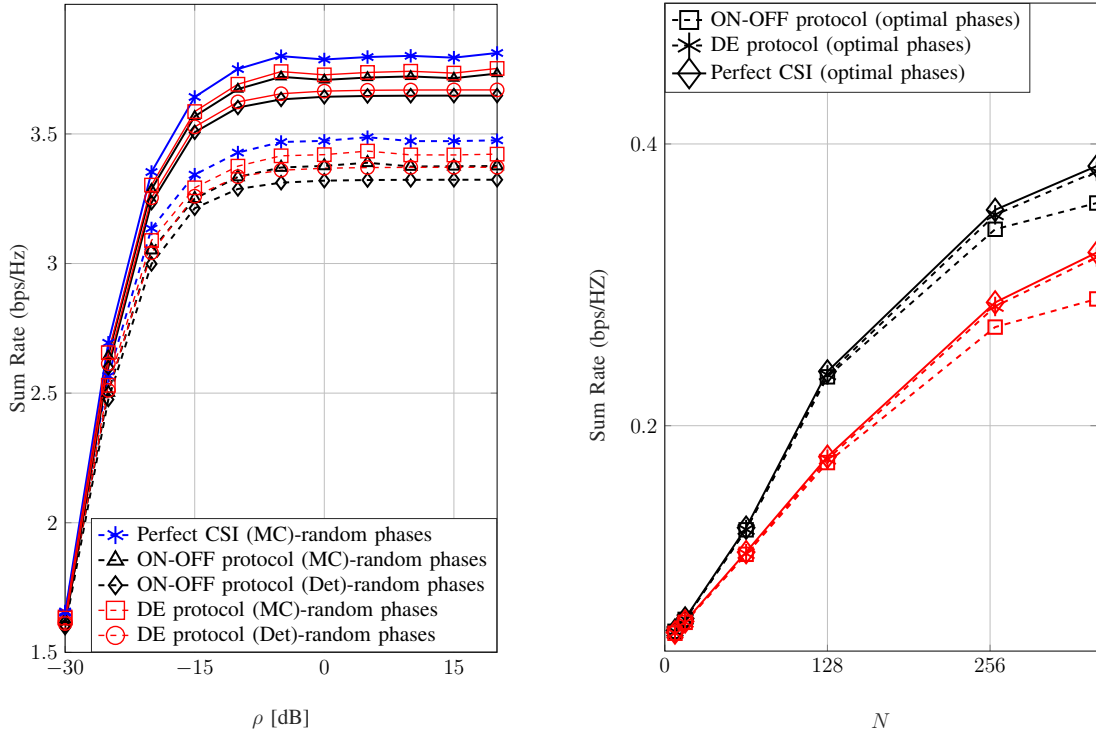
$$\gamma_k^{ray^\circ} = \frac{1}{\underbrace{\frac{1}{M} \sum_{l \neq k} \frac{\beta_{d,l}}{\beta_{d,k}}}_{\text{Interference}} + \underbrace{\frac{\sum_{l=1}^K \beta_{d,l}}{M \beta_{d,k}^2 \rho (cN + 1)}}_{\text{Noise}}}. \quad (47)$$

This corollary yields two important insights. First it verifies the ‘‘massive MIMO effect’’ observed in [25], that as M increases for fixed N and K , the user rates grows logarithmically. Second, the use of an RIS under Rayleigh fading $\mathbf{h}_{2,k}$ is only useful in large systems when the average received SNR is low, i.e. either ρ is low or the path loss is high which results in small $\beta_{d,k}$. This is often the case for cell-edge users. In such a noise-limited scenario³, the second term in the denominator of (47) will dominate the first and increasing N will produce a noticeable increase in the SINR values. In an interference-limited scenario, the use of an RIS yields no substantial benefit. This can be intuitively explained by noting that under Rayleigh fading RIS-to-user channels, the RIS only yields an array gain of N asymptotically. This gain appears in both the energy of desired and interfering signals and the net effect becomes negligible if the the interference is dominant.

V. SIMULATION RESULTS

In this section we provide simulation results to validate our results. We consider a multi-user setup in a 3D coordinate system where a BS equipped with M antennas communicates with K single antennas cell-edge users. The users are placed along an arc of radius 550m that spans angles from -30° to 30° with respect to the x -axis. Since the cell edge users have the most sensitive performance due to high path loss, we will focus on the performance of these users under RIS deployment. Using (x, y, z) coordinates (in meters), the BS and RIS are deployed at $(0, 0, 25)$ and $(\bar{x}, \bar{y}, 40)$ respectively where \bar{x} is the mean of the x coordinates of all users and \bar{y} is the mean of y coordinates of all users. We assume a full rank BS-to-RIS LoS channel matrix generated using the relationship in [13], [34]. Additionally, we define $p_k = 1/K$, $\forall k$ and $P_{max} = 1$. The path loss model is generally represented as $\beta_k = \frac{C_0}{d^\alpha}$, with C_0 set as 30dB. The

³Noise-limited here implies that the noise power is much higher than the intra-cell interference power. In multi-cell systems (not the focus of this work), the total noise consists of the noise plus inter-cell interference.



(a) Comparison of deterministic (Det) equivalents and Monte-Carlo (MC) simulations. Solid (dashed) lines illustrate optimal (random) RIS phases

(b) Deterministic equivalents under different protocols. Black (red) curves denote the performance under optimal (random) phases at the RIS.

Fig. 2: Sum rate versus ρ and N for a Rician fading channel under perfect and imperfect CSI.

path loss coefficient for BS-RIS LoS link is set as $\alpha = 2$. The path loss coefficient for RIS-user link i.e. $\beta_{2,k}$, is set as 2.8, and that for BS-user link, i.e. $\beta_{d,k}$, is set as 3.5 [10].

A. Simulation Results under Rician Fading

We will start with validating the tightness of the deterministic equivalents derived under Rician fading and both MMSE ON/OFF and MMSE DE protocols. For the purpose of this result, we let $\beta_{2,k} = c_k \beta_{d,k}$ and abstract $\frac{\beta_{2,k}}{\sigma^2}$ as ρ . Then, we plot in Fig. 2b against ρ , the sum-rate in (35) using the deterministic equivalent of the SINR in Theorem 2 for MMSE ON/OFF and the one in Theorem 3 for MMSE DE. We also plot the Monte-Carlo simulated sum-rate in (30) under perfect CSI as well as under both estimation protocols. The results are plotted against ρ for $M = N = K = 48$ and $\rho_{tr} = 8$ dB.

From Fig. 2a we can see that the deterministic equivalents provide a tight approximation to the Monte-Carlo simulated sum-rate for moderate values of M, K, N . These equivalents can therefore be used as an analytical tool to study the system performance without relying on time consuming

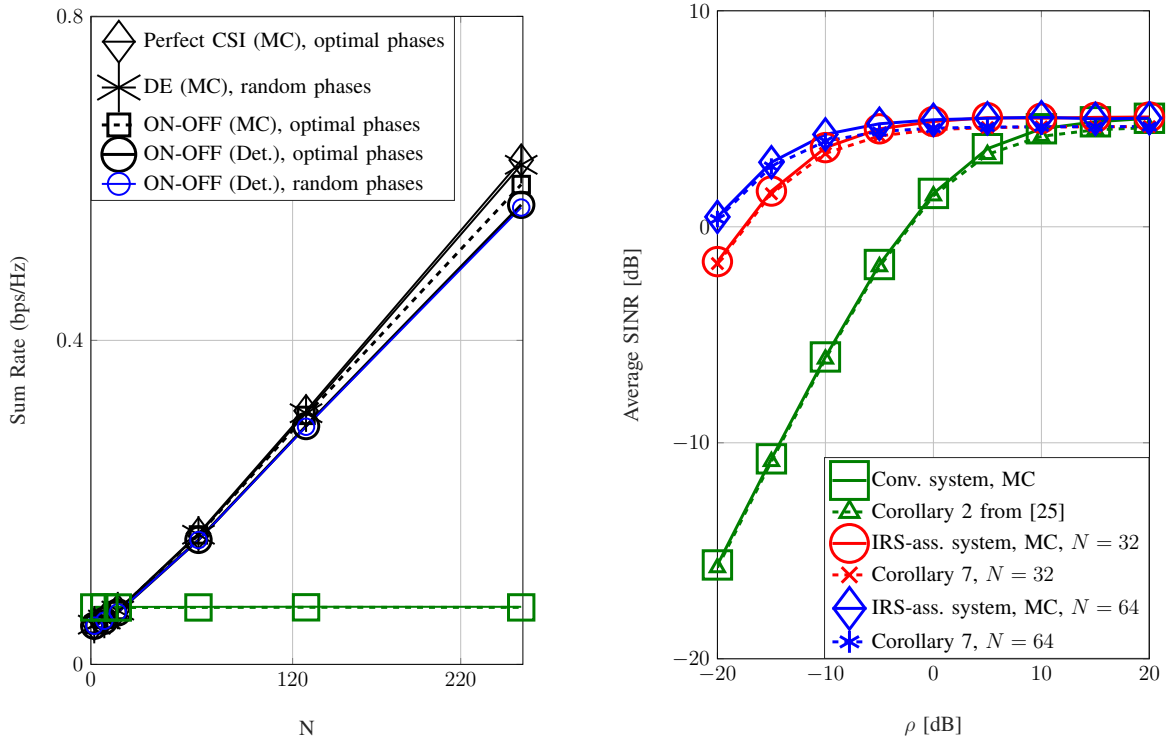
Monte-Carlo realizations. We also plot the curves under random RIS phases and compare it with system performance under optimized RIS phases. The curves illustrate the performance gain that can be realized in Rician environments by reflect beamforming through optimization of the phase shifts using Algorithm 1. We also observe that in terms of SINR, the MMSE-DE protocol yields a better sum-rate than MMSE-ON/OFF protocol, since the estimation of the overall channel \mathbf{h}_k^{ric} in the ON/OFF protocol suffers from errors in the estimation of $N + 1$ channel vectors. DE is therefore desirable, provided CSI of individual links is not needed to design the RIS, which is the case for large systems where the RIS phase-shifts are just designed using statistical CSI.

The following results illustrate the performance gain achieved by an RIS-assisted MISO system over a conventional MISO system in a Rician fading environment. In generating the results, we introduce the model for ρ_{tr} as $\rho_{tr} = \frac{p_c \tau_u}{\sigma^2}$, which depends on the noise variance in the uplink σ^2 set as 10^{-23} Joules as well as the pilot Tx power p_c set as 1W. The channel estimation period τ_u is defined as 0.01τ , where τ is the length of the coherence interval set as 10ms. Therefore the length of each channel estimation sub-phase is $\tau_s = \frac{0.01\tau}{(N+1)}$ under MMSE-ON/OFF protocol. Under the DE protocol, we will have $\tau_s = 0.01\tau$ as estimation is done in a single sub-phase. Also for the conventional MISO system where no RIS is deployed, we will have $\tau_s = 0.01\tau$. Under the block-fading channel model, the net achievable rate of user k is given as $R_k = (1 - \frac{\tau_u}{\tau}) \log_2(1 + \text{SINR}_k)$. The net achievable sum-rate is then given as $R_{sum} = \sum_{k=1}^K R_k$.

In Fig. 2b we plot the deterministic equivalent curves under perfect CSI and imperfect CSI for both ON-OFF protocol as well as DE protocol in the Rician fading environment. For this result, we have set $M = 40$, $N = \{8, 16, 128, 260, 340\}$ and $K = 28$. The figure illustrates the system's performance under both optimized RIS phases (black) and randomly generated RIS phases (red). Optimizing the RIS phase-shifts using the proposed projected gradient ascent algorithm yields significant reflect beamforming gains. It is also important to note that DE performs significantly better than ON/OFF protocol and the performance gap increases with N . This is because the length of each sub-phase used to estimate the channel vectors reduces linearly with N under MMSE-ON/OFF protocol resulting in poorer quality channel estimates, while the length of the single sub-phase used to estimate the overall channel under DE is unaffected by N .

B. Simulation Results under Rayleigh Fading

Next we plot results for the Rayleigh fading scenario. In Fig. 3a, we study the sum-rate achieved by $K = 40$ users in an RIS-assisted MISO system with $M = 40$ BS antennas against a



(a) Sum-rate versus N under optimal phases and random phases. Green lines represent the conventional MISO system (No RIS) under imperfect CSI (dashed line) and perfect CSI (solid line).

(b) Performance of RIS-assisted system under the channel in (47), where ρ is abstracted as $1/\sigma^2$.

Fig. 3: Sum rate and average SINR under Rayleigh fading.

varying number of RIS elements and compare the performance with that of a conventional MISO system with $M = 60$ BS antennas. The RIS phase-shifts are drawn randomly under MMSE-DE protocol given our observation from Theorem 5 that for large systems RIS phase-shifts do not appear in the deterministic equivalent of the SINR and therefore optimizing them yields no sum-rate gain under Rayleigh fading. Under the MMSE-ON/OFF protocol, we plot the sum-rate under both optimized RIS phase-shifts using Algorithm 1 where the gradient expression is given in Lemma 5, as well as random phase-shifts. We observe that with increasing number of RIS elements N , the RIS-assisted system outperforms the conventional large MISO system, by using a fewer number of active antennas at the BS. The result shows that the RIS-assisted system with 16 passive reflecting elements at the RIS and 40 active antennas at the BS can achieve the same performance as a conventional large MISO system with 60 active antennas, thus making it an energy-efficient alternative to technologies like Massive MIMO and network densification.

The results also verifies our observation made in Theorem 4 that the value of phase-shifts has negligible effect on the asymptotic sum-rate performance under Rayleigh fading. Optimizing the phase-shifts indeed made little to no effect in performance, as the blue and black curves with circle markers shown in Fig. 3a are very close. The gap between perfect and imperfect CSI curves increases significantly with N under MMSE-ON/OFF protocol as the quality of estimates deteriorates. DE is therefore a desirable estimation scheme when considering large systems.

Fig. 3b studies the performance of RIS-assisted system against ρ under the simplified channel model considered in Corollary 7 for perfect CSI. The result in (47) in Corollary 7 is also plotted and the match between the Monte-Carlo simulated average SINR and the theoretical result in Corollary 7 is very good. As discussed in Sec. III-C, RIS is only beneficial under large system dimensions and Rayleigh fading when ρ takes small to moderate values, i.e. the system is noise-limited, which is often the case for cell edge users and users in dense urban-macro settings. For interference-limited scenarios (i.e. high ρ), the performance of RIS-assisted system approaches that of the conventional MISO system under Rayleigh fading. Note that the conventional MISO system was studied under the model in (24) in [25].

VI. CONCLUSION

In this work, we studied the asymptotic sum-rate performance of an RIS-assisted MISO downlink system under both Rician fading and Rayleigh fading environments with imperfect CSI. We studied the system under two estimation protocols, namely the ON/OFF and DE channel estimation protocol, and derived the MMSE channel estimates under each protocol. Considering MRT precoding at the BS and an asymptotic system limit, we derived the closed-form expression of the achievable sum-rate under Rician and Rayleigh fading scenarios and under each estimation protocol. Results showed that under Rayleigh fading, RIS provides an array gain but negligible beamforming gain, while in Rician fading scenario RIS provides both array and beamforming gains. We used a projected gradient ascent algorithm to optimize the RIS phase-shifts, under both ON/OFF and DE estimation protocols. Numerical results showed the effect of RIS phase-shift optimization in Rician fading environments and also revealed that DE protocol outperforms ON/OFF protocol particularly for large RISs.

APPENDIX A

PROOF OF LEMMA 1

Given the observed training signal, $\mathbf{r}_{1,k}^{tr}$, in the first sub-interval of the channel estimation phase given in (13), we can write the MMSE estimate of $\hat{\mathbf{h}}_{d,k}^{NLoS}$ as

$$\hat{\mathbf{h}}_{d,k}^{NLoS} = \mathbf{W}(\mathbf{r}_{1,k}^{tr} - \bar{\mathbf{h}}_{d,k}), \quad (48)$$

where \mathbf{W} is found as the solution to $\min_{\mathbf{W}} \mathbb{E}[|\hat{\mathbf{h}}_{d,k}^{NLoS} - \mathbf{h}_{d,k}^{NLoS}|^2]$ and turns out to be $\mathbf{W} = \mathbb{E}[(\mathbf{r}_{1,k}^{tr} - \bar{\mathbf{h}}_{d,k})\mathbf{h}_{d,k}^{NLoS^H}](\mathbb{E}[(\mathbf{r}_{1,k}^{tr} - \bar{\mathbf{h}}_{d,k})(\mathbf{r}_{1,k}^{tr} - \bar{\mathbf{h}}_{d,k})^H])^{-1}$. Noting that $\mathbf{n}_{i,k}^{tr}$ and $\mathbf{h}_{d,k}^{NLoS}$ are independent random vectors, we obtain,

$$\mathbb{E}[(\mathbf{r}_{1,k}^{tr} - \bar{\mathbf{h}}_{d,k})\mathbf{h}_{d,k}^{NLoS^H}] = \mathbb{E}[(\mathbf{h}_{d,k}^{NLoS} + \mathbf{n}_{1,k}^{tr})\mathbf{h}_{d,k}^{NLoS^H}] = \mathbb{E}[\mathbf{h}_{d,k}^{NLoS}\mathbf{h}_{d,k}^{NLoS^H}] = \beta_{d,k}^{NLoS}\mathbf{I}_M. \quad (49)$$

Next we find $\mathbb{E}[(\mathbf{r}_{1,k}^{tr} - \bar{\mathbf{h}}_{d,k})^tr(\mathbf{r}_{1,k}^{tr} - \bar{\mathbf{h}}_{d,k})^H]$ as,

$$\mathbb{E}[(\mathbf{r}_{1,k}^{tr} - \bar{\mathbf{h}}_{d,k})(\mathbf{r}_{1,k}^{tr} - \bar{\mathbf{h}}_{d,k})^H] = \mathbb{E}[(\mathbf{h}_{d,k}^{NLoS} + \mathbf{n}_{1,k}^{tr})(\mathbf{h}_{d,k}^{NLoS} + \mathbf{n}_{1,k}^{tr})^H], \quad (50)$$

$$= \mathbb{E}[\mathbf{h}_{d,k}^{NLoS}\mathbf{h}_{d,k}^{NLoS^H}] + \mathbb{E}[\mathbf{n}_{1,k}^{tr}\mathbf{n}_{1,k}^{trH}] = \beta_{d,k}^{NLoS}\mathbf{I}_M + \frac{1}{\rho_{tr}}\mathbf{I}_M. \quad (51)$$

Putting these expression together, we obtain,

$$\hat{\mathbf{h}}_{d,k}^{NLoS} = \beta_{d,k}^{NLoS}\mathbf{I}_M \left(\beta_{d,k}^{NLoS}\mathbf{I}_M + \frac{1}{\rho_{tr}}\mathbf{I}_M \right)^{-1} (\mathbf{r}_{1,k}^{tr} - \bar{\mathbf{h}}_{d,k}) = \frac{\beta_{d,k}^{NLoS}}{\beta_{d,k}^{NLoS} + \frac{1}{\rho_{tr}}} (\mathbf{r}_{1,k}^{tr} - \bar{\mathbf{h}}_{d,k}). \quad (52)$$

This completes the derivation of (17).

The MMSE estimate of $\mathbf{h}_{0,k,i}^{NLoS}$ is obtained as,

$$\hat{\mathbf{h}}_{0,k,i}^{NLoS} = \mathbf{W}(\tilde{\mathbf{r}}_{i,k}^{tr} - \bar{\mathbf{h}}_{d,k} - \bar{\mathbf{h}}_{0,k,i}) \quad (53)$$

where $\mathbf{W} = \mathbb{E}[(\tilde{\mathbf{r}}_{i,k}^{tr} - \bar{\mathbf{h}}_{d,k} - \bar{\mathbf{h}}_{0,k,i})\mathbf{h}_{0,k,i}^{NLoS^H}](\mathbb{E}[(\tilde{\mathbf{r}}_{i,k}^{tr} - \bar{\mathbf{h}}_{d,k} - \bar{\mathbf{h}}_{0,k,i})(\tilde{\mathbf{r}}_{i,k}^{tr} - \bar{\mathbf{h}}_{d,k} - \bar{\mathbf{h}}_{0,k,i})^H])^{-1}$ and $\tilde{\mathbf{r}}_{i,k}^{tr}$ is given in (15).

We first find the expression of $\mathbb{E}[(\tilde{\mathbf{r}}_{i,k}^{tr} - \bar{\mathbf{h}}_{d,k} - \bar{\mathbf{h}}_{0,k,i})\mathbf{h}_{0,k,i}^{NLoS^H}]$ by noting that that $\mathbf{n}_{i,k}^{tr}$ and $\mathbf{h}_{0,k,i}^{NLoS}$ are independent random vectors, and $\tilde{\mathbf{h}}_{d,k}^{NLoS}$ and $\mathbf{h}_{0,k,i}^{NLoS}$ are independent random vectors.

Therefore,

$$\begin{aligned} \mathbb{E}[(\tilde{\mathbf{r}}_{i,k}^{tr} - \bar{\mathbf{h}}_{d,k} - \bar{\mathbf{h}}_{0,k,i})\mathbf{h}_{0,k,i}^{NLoS^H}] &= \mathbb{E}[(\tilde{\mathbf{h}}_{d,k}^{NLoS} + \mathbf{h}_{0,k,i}^{NLoS} + \mathbf{n}_{i,k}^{tr})\mathbf{h}_{0,k,i}^{NLoS^H}] = \mathbb{E}[\mathbf{h}_{0,k,i}^{NLoS}\mathbf{h}_{0,k,i}^{NLoS^H}] \\ &= \beta_{2,k}^{NLoS}\mathbf{h}_{1,i}\mathbf{h}_{1,i}^H. \end{aligned} \quad (54)$$

Next we find $\mathbb{E}[(\tilde{\mathbf{r}}_{i,k}^{tr} - \bar{\mathbf{h}}_{d,k} - \bar{\mathbf{h}}_{0,k,i})(\tilde{\mathbf{r}}_{i,k}^{tr} - \bar{\mathbf{h}}_{d,k} - \bar{\mathbf{h}}_{0,k,i})^H]$ by using the independence of $\mathbf{n}_{i,k}^{tr}$ and $\mathbf{h}_{0,k,i}^{NLoS}$, $\tilde{\mathbf{h}}_{d,k}^{NLoS}$ and $\mathbf{h}_{0,k,i}^{NLoS}$, and $\tilde{\mathbf{h}}_{d,k}^{NLoS}$ and $\mathbf{n}_{i,k}^{tr}$ to obtain

$$\mathbb{E}[(\tilde{\mathbf{r}}_{i,k}^{tr} - \bar{\mathbf{h}}_{d,k} - \bar{\mathbf{h}}_{0,k,i})(\tilde{\mathbf{r}}_{i,k}^{tr} - \bar{\mathbf{h}}_{d,k} - \bar{\mathbf{h}}_{0,k,i})^H] \quad (55)$$

$$= \mathbb{E}[\tilde{\mathbf{h}}_{d,k}^{NLoS}\tilde{\mathbf{h}}_{d,k}^{NLoS^H}] + \mathbb{E}[\mathbf{h}_{0,k,i}^{NLoS}\mathbf{h}_{0,k,i}^{NLoS^H}] + \mathbb{E}[\mathbf{n}_{i,k}^{tr}\mathbf{n}_{i,k}^{trH}] \quad (56)$$

$$= \mathbf{C}_{\tilde{\mathbf{h}}_{d,k}^{NLoS}\tilde{\mathbf{h}}_{d,k}^{NLoS^H}} + \beta_{2,k}^{NLoS}\mathbf{h}_{1,i}\mathbf{h}_{1,i}^H + \frac{1}{\rho_{tr}}\mathbf{I}_M. \quad (57)$$

To obtain $\mathbf{C}_{\hat{\mathbf{h}}_{d,k}^{NLoS} \hat{\mathbf{h}}_{d,k}^{NLoS^H}}$, we recall that $\tilde{\mathbf{h}}_{d,k}^{NLoS} = \mathbf{h}_{d,k}^{NLoS} - \hat{\mathbf{h}}_{d,k}^{NLoS}$ and therefore,

$$\mathbf{C}_{\hat{\mathbf{h}}_{d,k}^{NLoS} \hat{\mathbf{h}}_{d,k}^{NLoS^H}} \quad (58)$$

$$= \mathbb{E}[\mathbf{h}_{d,k}^{NLoS} \mathbf{h}_{d,k}^{NLoS^H}] - \mathbb{E}[\hat{\mathbf{h}}_{d,k}^{NLoS} \hat{\mathbf{h}}_{d,k}^{NLoS^H}], \quad (59)$$

$$= \beta_{d,k}^{NLoS} \mathbf{I}_M - \frac{\beta_{d,k}^{NLoS^2}}{(\beta_{d,k}^{NLoS} + \frac{1}{\rho_{tr}})^2} \mathbb{E}[(\mathbf{r}_{1,k}^{tr} - \bar{\mathbf{h}}_{d,k})(\mathbf{r}_{1,k}^{tr} - \bar{\mathbf{h}}_{d,k})^H], \quad (60)$$

$$= \beta_{d,k}^{NLoS} \mathbf{I}_M - \frac{\beta_{d,k}^{NLoS^2}}{(\beta_{d,k}^{NLoS} + \frac{1}{\rho_{tr}})^2} (\beta_{d,k}^{NLoS} + \frac{1}{\rho_{tr}}) \mathbf{I}_M = \frac{\beta_{d,k}^{NLoS}}{\beta_{d,k}^{NLoS} \rho_{tr} + 1} \mathbf{I}_M. \quad (61)$$

Therefore, putting (61) back in (57) and using it along with (54) in (53) we obtain, $\hat{\mathbf{h}}_{0,k,i}^{NLoS} = \beta_{2,k}^{NLoS} \mathbf{h}_{1,i} \mathbf{h}_{1,i}^H \left(\mathbf{C}_{\hat{\mathbf{h}}_{d,k}^{NLoS} \hat{\mathbf{h}}_{d,k}^{NLoS^H}} + \beta_{2,k}^{NLoS} \mathbf{h}_{1,i} \mathbf{h}_{1,i}^H + \frac{1}{\rho_{tr}} \mathbf{I}_M \right)^{-1} (\tilde{\mathbf{r}}_{i,k}^{tr} - \bar{\mathbf{h}}_{d,k} - \bar{\mathbf{h}}_{0,k,i})$. This completes the proof of (18).

APPENDIX B

PROOF OF THEOREM 1

Recall $\hat{\mathbf{h}}_k^{ric} = \hat{\mathbf{h}}_{d,k}^{NLoS} + \bar{\mathbf{h}}_{d,k} + \sum_{i=1}^N \hat{\mathbf{h}}_{0,k,i}^{NLoS} v_i + \sum_{i=1}^N \bar{\mathbf{h}}_{0,k,i} v_i$, with mean $\mathbb{E}[\hat{\mathbf{h}}_k^{ric}] = \bar{\mathbf{h}}_{d,k} + \sum_{i=1}^N \bar{\mathbf{h}}_{0,k,i} v_i$ and covariance matrix $\mathbb{E}[\hat{\mathbf{h}}_k^{ric} \hat{\mathbf{h}}_k^{ric^H}] - \mathbb{E}[\hat{\mathbf{h}}_k^{ric}] \mathbb{E}[\hat{\mathbf{h}}_k^{ric}]^H$. Noting that $\hat{\mathbf{h}}_{0,k,i}^{NLoS}$ and $\hat{\mathbf{h}}_{d,k}^{NLoS}$ are independent, we can define the covariance matrix as:

$$\mathbb{E}[\hat{\mathbf{h}}_k^{ric} \hat{\mathbf{h}}_k^{ric^H}] - \mathbb{E}[\hat{\mathbf{h}}_k^{ric}] \mathbb{E}[\hat{\mathbf{h}}_k^{ric}]^H = \mathbb{E}[\hat{\mathbf{h}}_{d,k}^{NLoS} \hat{\mathbf{h}}_{d,k}^{NLoS^H}] + \sum_{j=1}^N \sum_{i=1}^N v_i \mathbb{E}[\hat{\mathbf{h}}_{0,k,i}^{NLoS} \hat{\mathbf{h}}_{0,k,j}^{NLoS^H}] v_j^*, \quad (62)$$

where $\mathbb{E}[\hat{\mathbf{h}}_{d,k}^{NLoS} \hat{\mathbf{h}}_{d,k}^{NLoS^H}] = \frac{\beta_{d,k}^{NLoS^2}}{(\beta_{d,k}^{NLoS} + \frac{1}{\rho_{tr}})^2} \mathbb{E}[(\mathbf{r}_{1,k}^{tr} - \bar{\mathbf{h}}_{d,k})(\mathbf{r}_{1,k}^{tr} - \bar{\mathbf{h}}_{d,k})^H] = \frac{\beta_{d,k}^{NLoS^2}}{(\beta_{d,k}^{NLoS} + \frac{1}{\rho_{tr}})^2} (\beta_{d,k}^{NLoS} + \frac{1}{\rho_{tr}}) \mathbf{I}_M = \frac{\beta_{d,k}^{NLoS^2}}{\beta_{d,k}^{NLoS} + \frac{1}{\rho_{tr}}} \mathbf{I}_M$. We now compute $\sum_{j=1}^N \sum_{i=1}^N v_i \mathbb{E}[\hat{\mathbf{h}}_{0,k,i}^{NLoS} \hat{\mathbf{h}}_{0,k,j}^{NLoS^H}] v_j^*$ by using the expression of $\hat{\mathbf{h}}_{0,k,i}^{NLoS}$ from (18) and noting the independence between $\tilde{\mathbf{h}}_{d,k}^{NLoS}$, $\mathbf{h}_{0,k,i}^{NLoS}$ and $\mathbf{n}_{i,k}^{tr}$ as

$$\sum_{j=1}^N \sum_{i=1}^N v_i \mathbb{E}[\mathbf{R}_{0,i,k}^{NLoS} \mathbf{Q}_{i,k}^{NLoS} (\tilde{\mathbf{h}}_{d,k}^{NLoS} + \mathbf{h}_{0,k,i}^{NLoS} + \mathbf{n}_{i,k}^{tr}) (\tilde{\mathbf{h}}_{d,k}^{NLoS^H} + \mathbf{h}_{0,k,j}^{NLoS^H} + \mathbf{n}_{j,k}^{tr^H}) \mathbf{Q}_{j,k}^{NLoS^H} \mathbf{R}_{0,j,k}^{NLoS^H}] v_j^*. \quad (63)$$

By expanding (63) and applying the expectation on the independent terms, while using the fact that $\mathbb{E}[\mathbf{h}_{0,k,i}^{NLoS} \mathbf{h}_{0,k,j}^{NLoS^H}] = 0$ and $\mathbb{E}[\mathbf{n}_{i,k}^{tr} \mathbf{n}_{j,k}^{tr^H}] = 0$, for $i \neq j$, we obtain

$$\begin{aligned} & \sum_{j=1}^N \sum_{i=1}^N v_i \mathbb{E}[\hat{\mathbf{h}}_{0,k,i}^{NLoS} \hat{\mathbf{h}}_{0,k,j}^{NLoS^H}] v_j^* \\ &= \sum_{j=1}^N \sum_{i=1}^N v_i \mathbf{R}_{0,i,k}^{NLoS} \mathbf{Q}_{i,k}^{NLoS} \mathbf{C}_{\hat{\mathbf{h}}_{d,k}^{NLoS} \hat{\mathbf{h}}_{d,k}^{NLoS^H}} \mathbf{Q}_{j,k}^{NLoS^H} \mathbf{R}_{0,j,k}^{NLoS^H} v_j^* \\ &+ \sum_{i=1}^N \mathbf{R}_{0,i,k}^{NLoS} \mathbf{Q}_{i,k}^{NLoS} \mathbf{R}_{0,i,k}^{NLoS} \mathbf{Q}_{i,k}^{NLoS^H} \mathbf{R}_{0,i,k}^{NLoS^H} + \sum_{i=1}^N \mathbf{R}_{0,i,k}^{NLoS} \mathbf{Q}_{i,k}^{NLoS} \frac{1}{\rho_{tr}} \mathbf{I}_M \mathbf{Q}_{i,k}^H \mathbf{R}_{0,i,k}^{NLoS^H}. \end{aligned} \quad (64)$$

The expression can be simplified to obtain,

$$\begin{aligned}
& \sum_{j=1}^N \sum_{i=1}^N v_i \mathbb{E}[\hat{\mathbf{h}}_{0,k,i}^{NLoS} \hat{\mathbf{h}}_{0,k,j}^{NLoS^H}] v_j^* \\
&= \sum_{j=1}^N \sum_{i=1}^N v_i \mathbf{R}_{0,i,k}^{NLoS} \mathbf{Q}_{i,k}^{NLoS} \mathbf{C}_{\hat{\mathbf{h}}_{d,k}^{NLoS} \hat{\mathbf{h}}_{d,k}^{NLoS}} \mathbf{Q}_{j,k}^{NLoS^H} \mathbf{R}_{0,j,k}^{NLoS^H} v_j^* \\
&\quad + \sum_{i=1}^N \mathbf{R}_{0,i,k}^{NLoS} \mathbf{Q}_{i,k}^{NLoS} (\mathbf{R}_{0,i,k}^{NLoS} + \frac{1}{\rho_{tr}} \mathbf{I}_M) \mathbf{Q}_{i,k}^{NLoS^H} \mathbf{R}_{0,i,k}^{NLoS^H} \tag{65}
\end{aligned}$$

Putting (65) and $\mathbb{E}[\hat{\mathbf{h}}_{d,k}^{NLoS} \hat{\mathbf{h}}_{d,k}^{NLoS^H}] = \frac{\beta_{d,k}^{NLoS^2}}{\beta_{d,k}^{NLoS} + \frac{1}{\rho_{tr}}} \mathbf{I}_M$ together in (62) completes the proof of Theorem 1 by simply defining $\hat{\mathbf{h}}_k^{ric}$ as the sum of *LoS* terms and statistical representation of *NLoS* terms.

APPENDIX C

PROOF OF THEOREM 2

In this section we derive the deterministic equivalent of the SINR under Rician fading. The strategy is to divide both the numerator and denominator of the SINR expression in (29) by K and work separately on the four terms: 1) the scaled signal power $\frac{p_k}{K} |\mathbf{h}_k^{ric^H} \hat{\mathbf{h}}_k^{ric}|^2$, 2) the scaled interference power $\sum_{l \neq k} \frac{p_l}{K} |\mathbf{h}_k^{ric^H} \hat{\mathbf{h}}_l^{ric}|^2$, 3) the power normalization term $\frac{1}{K} \Psi$ and 4) the variance term $\frac{p_k}{K} \text{Var}[\mathbf{h}_k^{ric^H} \hat{\mathbf{h}}_k^{ric}]$. We will derive the deterministic equivalent for each of these terms separately and then obtain the final expression for $\gamma_k^{ric^\circ}$.

A. Deterministic equivalent of $\frac{1}{K} \mathbf{h}_k^{ric^H} \hat{\mathbf{h}}_k^{ric}$

Using the definitions in (9) and (19), we write

$$\begin{aligned}
& \frac{1}{K} \mathbf{h}_k^{ric^H} \hat{\mathbf{h}}_k^{ric} \\
&= \frac{1}{K} (\mathbf{h}_{d,k}^{NLoS} + \bar{\mathbf{h}}_{d,k} + \sum_{j=1}^N \hat{\mathbf{h}}_{0,k,j}^{NLoS} v_j + \sum_{j=1}^N \bar{\mathbf{h}}_{0,k,j} v_j)^H (\hat{\mathbf{h}}_{d,k}^{NLoS} + \bar{\mathbf{h}}_{d,k} + \sum_{i=1}^N \hat{\mathbf{h}}_{0,i,k}^{NLoS} v_i + \sum_{i=1}^N \bar{\mathbf{h}}_{0,i,k} v_i),
\end{aligned}$$

Noting that $\hat{\mathbf{h}}_{d,k}^{NLoS}$ and $\mathbf{h}_{0,k,i}^{NLoS}$ are independent vectors and applying [25, Lemma 4 (iii)], we have

$$\begin{aligned}
& \frac{1}{K} \mathbf{h}_k^{ric^H} \hat{\mathbf{h}}_k^{ric} - \frac{1}{K} \left(\text{tr} \mathbf{D}_k + \mathbf{h}_{d,k}^{NLoS^H} \hat{\mathbf{h}}_{d,k}^{NLoS} + \mathbf{h}_{d,k}^{NLoS^H} \sum_{i=1}^N \hat{\mathbf{h}}_{0,k,i}^{NLoS} v_i + \sum_{j=1}^N \sum_{i=1}^N v_j^H \mathbf{h}_{0,k,j}^{NLoS^H} \hat{\mathbf{h}}_{0,k,i}^{NLoS} v_i \right) \\
& \xrightarrow[M, N, K \rightarrow \infty]{a.s.} 0. \tag{66}
\end{aligned}$$

where $\mathbf{D}_k = \bar{\mathbf{h}}_{d,k} \bar{\mathbf{h}}_{d,k}^H + \bar{\mathbf{h}}_{d,k} (\sum_{i=1}^N v_i^* \bar{\mathbf{h}}_{0,k,i}^H) + (\sum_{i=1}^N \bar{\mathbf{h}}_{0,k,i} v_i) \bar{\mathbf{h}}_{d,k}^H + \sum_{j=1}^N \sum_{i=1}^N \bar{\mathbf{h}}_{0,k,i} v_i v_j^* \bar{\mathbf{h}}_{0,k,j}^H$.

We find the deterministic equivalents of the three non-deterministic terms in (66) separately.

Using (17), we obtain

$$\frac{1}{K} \mathbf{h}_{d,k}^{NLoS^H} \hat{\mathbf{h}}_{d,k}^{NLoS} = \frac{1}{K} \frac{\beta_{d,k}^{NLoS}}{\beta_{d,k}^{NLoS} + \frac{1}{\rho_{tr}}} \mathbf{h}_{d,k}^{NLoS^H} (\mathbf{h}_{d,k}^{NLoS} + \mathbf{n}_1^{tr}) \quad (67)$$

Next we notice the independence between \mathbf{n}_1^{tr} and $\mathbf{h}_{d,k}^{NLoS^H}$ and apply [25, Lemma 4 (iii)] to obtain,

$$\frac{1}{K} \mathbf{h}_{d,k}^{NLoS^H} \hat{\mathbf{h}}_{d,k}^{NLoS} - \frac{1}{K} \frac{\beta_{d,k}^{NLoS}}{\beta_{d,k}^{NLoS} + \frac{1}{\rho_{tr}}} \mathbf{h}_{d,k}^{NLoS^H} \mathbf{h}_{d,k}^{NLoS} \xrightarrow[M, N, K \rightarrow \infty]{a.s.} 0, \quad (68)$$

Given $\mathbf{h}_{d,k} \sim \mathcal{CN}(\mathbf{0}, \beta_{d,k}^{NLoS} \mathbf{I}_M)$, we apply [25, Lemma 4 (ii)] to obtain,

$$\frac{1}{K} \mathbf{h}_{d,k}^{NLoS^H} \hat{\mathbf{h}}_{d,k}^{NLoS} - \frac{1}{K} \frac{\beta_{d,k}^{NLoS^2} M}{\beta_{d,k}^{NLoS} + \frac{1}{\rho_{tr}}} \xrightarrow[M, N, K \rightarrow \infty]{a.s.} 0. \quad (69)$$

The second non-deterministic term in (66) is given using (18) as

$$\frac{1}{K} \sum_{j=1}^N \mathbf{h}_{d,k}^{NLoS^H} \hat{\mathbf{h}}_{0,k,j}^{NLoS} v_j = \frac{1}{K} \sum_{j=1}^N \mathbf{h}_{d,k}^{NLoS^H} (\mathbf{R}_{0,j,k}^{NLoS} \mathbf{Q}_{j,k}^{NLoS} \tilde{\mathbf{r}}_{j,k}^{tr}) v_j, \quad (70)$$

$$= \frac{1}{K} \sum_{j=1}^N \mathbf{h}_{d,k}^{NLoS^H} (\mathbf{R}_{0,j,k}^{NLoS} \mathbf{Q}_{j,k}^{NLoS} (\tilde{\mathbf{h}}_{d,k}^{NLoS} + \mathbf{h}_{0,k,j}^{NLoS} + \mathbf{n}_j^{tr})) v_j \quad (71)$$

We note that $\mathbf{h}_{d,k}^{NLoS^H}$ is independent of $\mathbf{h}_{0,k,j}^{NLoS}$ and \mathbf{n}_j^{tr} . Moreover, we recall that $\mathbf{h}_{d,k}^{NLoS} = \tilde{\mathbf{h}}_{d,k}^{NLoS} + \hat{\mathbf{h}}_{d,k}^{NLoS}$ and notice that $\hat{\mathbf{h}}_{d,k}^{NLoS}$ and $\tilde{\mathbf{h}}_{d,k}^{NLoS}$ are independent. Under these observations, we apply [25, Lemma 4 (iii)] successively to obtain

$$\frac{1}{K} \sum_{j=1}^N \mathbf{h}_{d,k}^{NLoS^H} \mathbf{R}_{0,j,k}^{NLoS} \mathbf{Q}_{j,k}^{NLoS} \tilde{\mathbf{h}}_{d,k}^{NLoS} v_j - \frac{1}{K} \sum_{j=1}^N \tilde{\mathbf{h}}_{d,k}^{NLoS^H} \mathbf{R}_{0,j,k}^{NLoS} \mathbf{Q}_{j,k}^{NLoS} \tilde{\mathbf{h}}_{d,k}^{NLoS} v_j \xrightarrow[M, N, K \rightarrow \infty]{a.s.} 0.$$

Next we apply the trace lemma on the quadratic term in $\tilde{\mathbf{h}}_{d,k}^{NLoS}$ where $\tilde{\mathbf{h}}_{d,k}^{NLoS} \sim \mathcal{CN}(\mathbf{0}, \mathbf{C}_{\tilde{\mathbf{h}}_{d,k}^{NLoS} \tilde{\mathbf{h}}_{d,k}^{NLoS^H}})$, where $\mathbf{C}_{\tilde{\mathbf{h}}_{d,k}^{NLoS} \tilde{\mathbf{h}}_{d,k}^{NLoS^H}}$ is defined in Lemma 1. The resulting convergence is given as

$$\frac{1}{K} \sum_{j=1}^N \mathbf{h}_{d,k}^{NLoS^H} \hat{\mathbf{h}}_{0,k,j}^{NLoS} v_j - \frac{1}{K} \sum_{j=1}^N \text{tr}(\mathbf{C}_{\tilde{\mathbf{h}}_{d,k}^{NLoS} \tilde{\mathbf{h}}_{d,k}^{NLoS^H}} \mathbf{R}_{0,j,k}^{NLoS} \mathbf{Q}_{j,k}^{NLoS}) v_j \xrightarrow[M, N, K \rightarrow \infty]{a.s.} 0. \quad (72)$$

Next we work out the deterministic equivalent of the third term using the definition of $\hat{\mathbf{h}}_{0,k,j}^{NLoS}$ from (18) as $\sum_{j=1}^N \sum_{i=1}^N v_i^* \mathbf{h}_{0,k,i}^{NLoS^H} \hat{\mathbf{h}}_{0,k,j}^{NLoS} v_j = \sum_{j=1}^N \sum_{i=1}^N v_i^* \mathbf{h}_{0,k,i}^{NLoS^H} (\mathbf{R}_{0,j,k}^{NLoS} \mathbf{Q}_{j,k}^{NLoS} (\tilde{\mathbf{h}}_{d,k}^{NLoS} + \mathbf{h}_{0,k,j}^{NLoS} + \frac{\mathbf{n}_j^{tr}}{\rho_{tr}})) v_j$. Noting that $\mathbf{h}_{0,k,i}^{NLoS}$ is independent of $\tilde{\mathbf{h}}_{d,k}$ and $\mathbf{n}_j^{tr} \forall i, j$, and independent of $\mathbf{h}_{0,k,j}^{NLoS}$ for $j \neq i$, we apply Lemma [25, Lemma 4 (iii)] to obtain

$$\frac{1}{K} \sum_{j=1}^N \sum_{i=1}^N v_i^* \mathbf{h}_{0,k,i}^{NLoS^H} \hat{\mathbf{h}}_{0,k,j}^{NLoS} v_j - \frac{1}{K} \sum_{i=1}^N v_i^* v_i \mathbf{h}_{0,k,i}^{NLoS^H} \mathbf{R}_{0,i,k}^{NLoS} \mathbf{Q}_{i,k}^{NLoS} \mathbf{h}_{0,k,i}^{NLoS} \xrightarrow[M, N, K \rightarrow \infty]{a.s.} 0. \quad (73)$$

Noting that $v_i^* v_i = 1$ and applying [25, Lemma 4 (ii)] on the quadratic term in $\mathbf{h}_{0,k,i}$ we obtain

$$\frac{1}{K} \sum_{i=1}^N \mathbf{h}_{0,k,i}^{NLoS^H} \mathbf{R}_{0,i,k}^{NLoS} \mathbf{Q}_{i,k}^{NLoS} \mathbf{h}_{0,k,i}^{NLoS} - \frac{1}{K} \sum_{i=1}^N \text{tr}(\mathbf{R}_{0,i,k}^{NLoS} \mathbf{R}_{0,i,k}^{NLoS} \mathbf{Q}_{i,k}^{NLoS}) \xrightarrow[M, N, K \rightarrow \infty]{a.s.} 0. \quad (74)$$

Therefore putting (69), (72) and (74) together in (66) we obtain

$$\begin{aligned} & \frac{1}{K} \mathbf{h}_k^{ricH} \hat{\mathbf{h}}_k^{ric} - \\ & \frac{1}{K} \text{tr} \left(\mathbf{D}_k + \frac{\beta_{d,k}^{NLoS^2}}{\beta_{d,k}^{NLoS} + \frac{1}{\rho_{tr}}} \mathbf{I}_M + \sum_{i=1}^N \mathbf{C}_{\hat{\mathbf{h}}_{d,k}^{NLoS} \hat{\mathbf{h}}_{d,k}^{NLoSH}} \mathbf{R}_{0,i,k}^{NLoS} \mathbf{Q}_{i,k}^{NLoS} v_i + \mathbf{R}_{0,i,k}^{NLoS} \mathbf{R}_{0,i,k}^{NLoS} \mathbf{Q}_{i,k}^{NLoS} \right) \\ & \xrightarrow[M, N, K \rightarrow \infty]{a.s.} 0. \end{aligned}$$

B. Deterministic equivalent of $\frac{1}{K} \sum_{l \neq k} p_l |\mathbf{h}_k^H \hat{\mathbf{h}}_l|^2$

Note that $\frac{1}{K} \sum_{l \neq k} p_l |\mathbf{h}_k^{ricH} \hat{\mathbf{h}}_l^{ric}|^2 = \frac{1}{K} \mathbf{h}_k^{ricH} \hat{\mathbf{H}}_{[k]}^{ricH} \mathbf{P}_{[k]} \hat{\mathbf{H}}_{[k]}^{ric} \mathbf{h}_k^{ric}$, where $\hat{\mathbf{H}}_{[k]}^{ric}$ is defined as $\hat{\mathbf{H}}_{[k]}^{ric} = [\hat{\mathbf{h}}_1^{ric}, \dots, \hat{\mathbf{h}}_{k-1}^{ric}, \hat{\mathbf{h}}_{k+1}^{ric}, \dots, \hat{\mathbf{h}}_K^{ric}]^H$. Note that $\hat{\mathbf{H}}_{[k]}^{ricH} \mathbf{P}_{[k]} \hat{\mathbf{H}}_{[k]}^{ric}$ is independent of \mathbf{h}_k^{ric} . Moreover \mathbf{h}_k^{ric} defined in (9) is distributed as $\mathcal{CN} \sim (\bar{\mathbf{h}}_{d,k} + \sum_{i=1}^N \bar{\mathbf{h}}_{0,k,i} v_i, \mathbf{A}_k^{ric})$ where \mathbf{A}_k^{ric} is defined in (9).

Using these observations, we apply [25, Lemma 4 (ii)] to obtain

$$\frac{1}{K} \mathbf{h}_k^{ricH} \hat{\mathbf{H}}_{[k]}^{ricH} \mathbf{P}_{[k]} \hat{\mathbf{H}}_{[k]}^{ric} \mathbf{h}_k^{ric} - \frac{1}{K} \text{tr}((\mathbf{D}_k + \mathbf{A}_k^{ric}) \hat{\mathbf{H}}_{[k]}^{ricH} \mathbf{P}_{[k]} \hat{\mathbf{H}}_{[k]}^{ric}) \xrightarrow[M, N, K \rightarrow \infty]{a.s.} 0 \quad (75)$$

Note that $\text{tr}((\mathbf{D}_k + \mathbf{A}_k^{ric}) \hat{\mathbf{H}}_{[k]}^{ricH} \mathbf{P}_{[k]} \hat{\mathbf{H}}_{[k]}^{ric}) = \sum_{l \neq k} p_l \hat{\mathbf{h}}_l^{ricH} (\mathbf{D}_k + \mathbf{A}_k^{ric}) \hat{\mathbf{h}}_l^{ric}$. Applying [25, Lemma 4 (ii)] on the quadratic form in $\hat{\mathbf{h}}_l^{ric}$ defined in (24), we obtain

$$\frac{1}{K} \sum_{l \neq k} p_l \hat{\mathbf{h}}_l^{ricH} (\mathbf{D}_k + \mathbf{A}_k^{ric}) \hat{\mathbf{h}}_l^{ric} - \frac{1}{K} \sum_{l \neq k} p_l \text{tr}((\mathbf{D}_k + \mathbf{C}_l^{ric})(\mathbf{D}_l + \mathbf{A}_k^{ric})) \xrightarrow[M, N, K \rightarrow \infty]{a.s.} 0 \quad (76)$$

where \mathbf{C}_l^{ric} is defined in Theorem 1 (20).

Therefore we obtain

$$\frac{1}{K} \sum_{l \neq k} p_l |\mathbf{h}_k^{ricH} \hat{\mathbf{h}}_l^{ric}|^2 - \frac{1}{K} \sum_{l \neq k} p_l \text{tr}((\mathbf{D}_l + \mathbf{C}_l^{ric})(\mathbf{D}_k + \mathbf{A}_k^{ric})) \xrightarrow[M, N, K \rightarrow \infty]{a.s.} 0 \quad (77)$$

C. Deterministic equivalent of $\frac{1}{K} \Psi = \frac{1}{K} \text{tr}(\mathbf{P} \mathbf{H}^{ric} \hat{\mathbf{H}}^{ricH})$

Note that $\frac{1}{K} \Psi$ can be written as $\frac{1}{K} \Psi = \sum_{k=1}^K p_k \hat{\mathbf{h}}_k^{ricH} \hat{\mathbf{h}}_k^{ric}$. Applying the [25, Lemma 4 (ii)] on the quadratic form in $\hat{\mathbf{h}}_l^{ric}$, we obtain

$$\frac{1}{K} \sum_{k=1}^K p_k \hat{\mathbf{h}}_k^{ricH} \hat{\mathbf{h}}_k^{ric} - \frac{1}{K} \sum_{k=1}^K p_k \text{tr}(\mathbf{D}_k + \mathbf{C}_k^{ric}) \xrightarrow[M, N, K \rightarrow \infty]{a.s.} 0. \quad (78)$$

D. Deterministic equivalent of $\frac{p_k}{K} \text{Var}[\mathbf{h}_k^H \hat{\mathbf{h}}_k]$

Note that $\frac{p_k}{K} \text{Var}[\mathbf{h}_k^{ricH} \hat{\mathbf{h}}_k^{ric}] = \text{Var}(x+y)$, where $x = \frac{p_k}{K} \mathbf{h}_k^{ricH} \hat{\mathbf{h}}_{d,k}^{NLoS}$ and $y = \frac{p_k}{K} \mathbf{h}_k^{ricH} \sum_{i=1}^N \hat{\mathbf{h}}_{0,k,i}^{NLoS} v_i$. It can be seen that $\text{Var}(x+y) \leq 2\text{Var}(x) + 2\text{Var}(y)$. The variance of x is bounded by $\mathbb{E}[|x|^2]$ which converges to 0. To see this note that $\frac{p_k}{K} \mathbf{h}_k^{ricH} \hat{\mathbf{h}}_{d,k}^{NLoS} - \frac{p_k}{K} \frac{\beta_{d,k}^{NLoS^2}}{\beta_{d,k}^{NLoS} + \frac{1}{\rho_{tr}}} \text{tr}(\mathbf{I}_M)$ using the definition of $\hat{\mathbf{h}}_{d,k}^{NLoS}$ in (17) and applying [25, Lemma 4 (iii)] on the independent vectors $\hat{\mathbf{h}}_{d,k}^{NLoS}$, $\mathbf{n}_{1,k}^{tr}$, $\mathbf{h}_{0,k,i}^{NLoS}$, and [25, Lemma 4 (ii)] on the quadratic term in $\mathbf{h}_{d,k}^{NLoS} \sim \mathcal{CN}(\mathbf{0}, \beta_{d,k}^{NLoS} \mathbf{I}_M)$. Then

$\mathbb{E}[|x|^2] = \frac{p_k^2 M^2}{K^2} \left(\frac{\beta_{d,k}^{NLoS^2}}{\beta_{d,k}^{NLoS} + \frac{1}{\rho_{tr}}} \right)^2 + o(1)$. Under Assumption 3 that p_k is of order $O(\frac{1}{K})$, we can see that $\mathbb{E}[|x|^2] \xrightarrow[M, K \rightarrow \infty]{a.s.} 0$. The variance of y can also be proved to converge to zero similarly. Therefore $\frac{p_k}{K} \text{Var}[\mathbf{h}_k^{ricH} \hat{\mathbf{h}}_k^{ric}] \xrightarrow[M, K \rightarrow \infty]{a.s.} 0$. Combining the results of these subsections completes the proof of Theorem 2.

REFERENCES

- [1] B. Al-Nahhas, Q.-U.-A. Nadeem, and A. Chaaban, "Intelligent reflecting surface assisted MISO downlink: Channel estimation and asymptotic analysis," in *IEEE Global Commun. Conf. (GLOBECOM)*, 2020, pp. 1–6.
- [2] S. Buzzi, C. I. T. E. Klein, H. V. Poor, C. Yang, and A. Zappone, "A survey of energy-efficient techniques for 5G networks and challenges ahead," *IEEE J. Sel. Areas in Commun.*, vol. 34, no. 4, pp. 697–709, April 2016.
- [3] Q. Wu, G. Y. Li, W. Chen, D. W. K. Ng, and R. Schober, "An overview of sustainable green 5G networks," *IEEE Wireless Commun.*, vol. 24, no. 4, pp. 72–80, Aug 2017.
- [4] Q. Wu and R. Zhang, "Towards smart and reconfigurable environment: Intelligent reflecting surface aided wireless network," *IEEE Commun. Mag.*, vol. 58, no. 1, pp. 106–112, 2020.
- [5] M. Di Renzo *et al.*, "Smart radio environments empowered by reconfigurable AI meta-surfaces: an idea whose time has come," *EURASIP J. Wireless Commun. Network*, vol. 2019, Dec. 2019.
- [6] E. Basar, M. Di Renzo, J. De Rosny, M. Debbah, M.-S. Alouini, and R. Zhang, "Wireless communications through reconfigurable intelligent surfaces," *IEEE Access*, vol. 7, pp. 116 753–116 773, 2019.
- [7] M. Di Renzo, A. Zappone, M. Debbah, M.-S. Alouini, C. Yuen, J. de Rosny, and S. Tretyakov, "Smart radio environments empowered by reconfigurable intelligent surfaces: How it works, state of research, and the road ahead," *IEEE J. Sel. Areas Commun.*, vol. 38, no. 11, pp. 2450–2525, 2020.
- [8] Y. Liu, X. Liu, X. Mu, T. Hou, J. Xu, M. Di Renzo, and N. Al-Dhahir, "Reconfigurable intelligent surfaces: Principles and opportunities," *IEEE Commun. Surv.*, pp. 1–1, 2021.
- [9] C. Huang, A. Zappone, M. Debbah, and C. Yuen, "Achievable rate maximization by passive intelligent mirrors," in *IEEE Int. Conf. Acoust., Speech and Signal Process. (ICASSP)*, April 2018, pp. 3714–3718.
- [10] Q. Wu and R. Zhang, "Intelligent reflecting surface enhanced wireless network via joint active and passive beamforming," *IEEE Trans. Wireless Commun.*, vol. 18, no. 11, pp. 5394–5409, Nov 2019.
- [11] Q. Wu and R. Zhang, "Intelligent reflecting surface enhanced wireless network: Joint active and passive beamforming design," in *Proc. IEEE Glob. Commun. Conf. (GLOBECOM)*, 2018, pp. 1–6.
- [12] —, "Beamforming optimization for intelligent reflecting surface with discrete phase shifts," in *IEEE Int. Conf. Acoust., Speech and Signal Process. (ICASSP)*, 2019, pp. 7830–7833.
- [13] Q.-U.-A. Nadeem, A. Kammoun, A. Chaaban, M. Debbah, and M.-S. Alouini, "Asymptotic max-min SINR analysis of reconfigurable intelligent surface assisted MISO systems," *IEEE Trans. Wireless Commun.*, 2020.
- [14] S. Li, B. Duo, X. Yuan, Y.-C. Liang, and M. Di Renzo, "Reconfigurable intelligent surface assisted UAV communication: Joint trajectory design and passive beamforming," *IEEE Wireless Commun. Let.*, vol. 9, no. 5, pp. 716–720, 2020.
- [15] X. Mu, Y. Liu, L. Guo, J. Lin, and N. Al-Dhahir, "Exploiting intelligent reflecting surfaces in NOMA networks: Joint beamforming optimization," *IEEE Trans. Wireless Commun.*, vol. 19, no. 10, p. 6884–6898, Oct 2020. [Online]. Available: <http://dx.doi.org/10.1109/TWC.2020.3006915>
- [16] X. Tan, Z. Sun, J. M. Jornet, and D. Pados, "Increasing indoor spectrum sharing capacity using smart reflect-array," in *IEEE Int. Conf. Commun. (ICC)*, May 2016, pp. 1–6.

- [17] X. Tan, Z. Sun, D. Koutsonikolas, and J. M. Jornet, "Enabling indoor mobile millimeter-wave networks based on smart reflect-arrays," in *IEEE Conf. Comp. Commun. (INFOCOM)*, April 2018, pp. 270–278.
- [18] D. Mishra and H. Johansson, "Channel estimation and low-complexity beamforming design for passive intelligent surface assisted MISO wireless energy transfer," in *IEEE Int. Conf. Acoust., Speech and Signal Process. (ICASSP)*, May 2019, pp. 4659–4663.
- [19] T. L. Jensen and E. De Carvalho, "An optimal channel estimation scheme for intelligent reflecting surfaces based on a minimum variance unbiased estimator," in *IEEE Int. Conf. Acoust., Speech and Signal Process. (ICASSP)*, 2020, pp. 5000–5004.
- [20] C. You, B. Zheng, and R. Zhang, "Intelligent Reflecting Surface with Discrete Phase Shifts: Channel Estimation and Passive Beamforming," *arXiv e-prints*, p. arXiv:1911.03916, Nov. 2019.
- [21] J. Chen, Y.-C. Liang, H. V. Cheng, and W. Yu, "Channel Estimation for Reconfigurable Intelligent Surface Aided Multi-User MIMO Systems," *arXiv e-prints*, p. arXiv:1912.03619, Dec 2019.
- [22] Z. He and X. Yuan, "Cascaded channel estimation for large intelligent metasurface assisted massive MIMO," *IEEE Wireless Commun. Lett.*, pp. 1–1, 2019.
- [23] Q.-U.-A. Nadeem, A. Kammoun, A. Chaaban, M. Debbah, and M.-S. Alouini, "Intelligent Reflecting Surface Assisted Wireless Communication: Modeling and Channel Estimation," *arXiv e-prints*, p. arXiv:1906.02360, Jun. 2019.
- [24] Q. Nadeem, A. Kammoun, M. Debbah, and M. Alouini, "Asymptotic analysis of RZF over double scattering channels with MMSE estimation," *IEEE Trans. Wireless Commun.*, vol. 18, no. 5, pp. 2509–2526, May 2019.
- [25] J. Hoydis, S. ten Brink, and M. Debbah, "Massive MIMO in the UL/DL of cellular networks: How many antennas do we need?" *IEEE J. Sel. Areas Commun.*, vol. 31, no. 2, pp. 160–171, 2013.
- [26] D. Mishra and H. Johansson, "Efficacy of multiuser massive MISO wireless energy transfer under iq imbalance and channel estimation errors over rician fading," *IEEE Int. Conf. Acoust., Speech and Signal Process. (ICASSP)*, pp. 3844–3848, 2018.
- [27] J. Jose, A. Ashikhmin, T. L. Marzetta, and S. Vishwanath, "Pilot contamination and precoding in multi-cell tdd systems," *IEEE Trans. Wireless Commun.*, vol. 10, no. 8, pp. 2640–2651, 2011.
- [28] T. Badloe, J. Mun, and J. Rho, "Metasurfaces-based absorption and reflection control: Perfect absorbers and reflectors," *Journal of Nanomaterials*, vol. 2017, pp. 1–18, 11 2017.
- [29] A. Epstein and G. V. Eleftheriades, "Synthesis of passive lossless metasurfaces using auxiliary fields for reflectionless beam splitting and perfect reflection," *Phys. Rev. Lett.*, vol. 117, p. 256103, Dec 2016.
- [30] R. Couillet and M. Debbah, *Random Matrix Methods for Wireless Communications*. Cambridge University Press, 2011.
- [31] S. Boyd and L. Vandenberghe, *Convex Optimization*. New York, NY, USA: Cambridge University Press, 2004.
- [32] K. B. Petersen and M. S. Pedersen, "The matrix cookbook," Oct. 2008, version 20081110. [Online]. Available: <http://www2.imm.dtu.dk/pubdb/p.php?3274>
- [33] W. Wang and W. Zhang, "Joint beam training and positioning for intelligent reflecting surfaces assisted millimeter wave communications," *IEEE Trans. Wireless Commun.*, pp. 1–1, 2021.
- [34] Q. Nadeem, A. Kammoun, M. Debbah, and M. Alouini, "A generalized spatial correlation model for 3D MIMO channels based on the fourier coefficients of power spectrums," *IEEE Trans. Signal Process.*, vol. 63, no. 14, pp. 3671–3686, July 2015.